

29 NASA CR-66279

INVESTIGATION OF THE ADHESION OF METALS
IN ULTRA-HIGH VACUUM

M. J. Hordon
J. R. Roehrig

December 1966/0

Distribution of this report is provided in the interest of information exchange. Responsibility for the contents resides in the author or organization that prepared it.

FACILITY FORM 602	N 67-22884	
	(ACCESSION NUMBER)	(THRU)
	10.52 RS 22-25	1
	(PAGES)	(CODE)
	CR-66279	17
	(NASA CR OR TMX OR AD NUMBER)	(CATEGORY)

Prepared under Contract No. NAS1-2691, Task #7 by
2 Norton Exploratory Research Division 3
1 NATIONAL RESEARCH CORPORATION
Cambridge, Massachusetts 2

for

NATIONAL AERONAUTICS AND SPACE ADMINISTRATION

ABSTRACT

Adhesion-friction tests were conducted at vacuum levels below 1×10^{-9} torr for annealed copper, titanium and tungsten. Prior to contact under loads up to 1000 lbs, mating cup-and-cone shaped specimens were subjected to xenon ion gas bombardment or rotational self-abrasion. Subsequently, residual shear torque, frictional torque, and normal adhesion forces were measured.

TABLE OF CONTENTS

	<u>PAGE</u>
PREFACE	v
SUMMARY	1
INTRODUCTION	2
ADHESION APPARATUS	3
Vacuum Chamber	3
Loading Mechanism	4
Specimen Heating Unit	11
Ion Beam Gun	11
Specimen Design	14
EXPERIMENTAL TECHNIQUE	14
Specimen Preparation	14
Vacuum Procedure	16
Ion Bombardment	17
Rotary Abrasion	17
Test Procedure	18
EXPERIMENTAL RESULTS	20
Ion Bombardment Tests	20
Rotary Abrasion Tests	21
Residual Adhesion Tests at Elevated Temperatures	27
Shear Friction Tests at Elevated Temperatures	30
Diffusion Bonding at Elevated Temperatures	36
DISCUSSION	37
Ion Bombardment Experiments	37
Rotary Abrasion Tests	39
Effect of Temperature on Adhesion Shear Forces	40
Frictional Effects	42
CONCLUSIONS	43
FUTURE WORK	44
REFERENCES	46

LIST OF ILLUSTRATIONS

<u>FIG. NO.</u>		<u>PAGE</u>
1	Adhesion Apparatus	5
2	Vacuum System for Adhesion Apparatus	6
3	Lower Loading System	7
4	Upper Loading Assembly	9
5	Adhesion Specimens Mounting Assembly	10
6	Illustration of Specimen Heating Unit	12
7	Ion Gun	13
8	Adhesion Test Specimen Couple	15
9	Variation of the Frictional Shear Torque with Compressive Load After Xe ⁺ Ion Bombardment	22
10	Variation of the Frictional Shear Torque with Compressive Load After Rotary Self- Abrasion	24
11	Variation of the Rotational Shear Torque with Abrasive Load for Titanium	25
12	Variation of the Rotational Shear Torque with Abrasive Load for Tungsten	26
13	Variation of the Rotational Shear Torque with Abrasive Load for Copper	28
14	Temperature Dependence of the Residual Adhesion Force After Rotary Abrasion	29
15	Dependence of the Residual Shear Torque on Abrasive Load at Constant Time for Selected Temperature Levels	31

<u>FIG. NO.</u>		<u>PAGE</u>
16	Increase in Residual Shear Torque with Abrasion Time at 500°C at Selected Abrasive Loads.	32
17	Temperature Dependence of the Frictional Torque with Compressive Load After Rota- tional Abrasion for Titanium	34
18	Temperature Dependence of the Frictional Torque with Compressive Load After Rota- tional Abrasion for Tungsten	35
19	Time-Temperature Dependence of the Re- sidual Adhesion Torque After 1000 lbs Loading.	38

PREFACE

This is the Summary Technical Report covering the work performed by National Research Corporation under Contract No. NAS1-2691, Task 7 for the National Aeronautics and Space Administration during the period June 29, 1965 to October 29, 1966. The program is a continuation of an investigation to examine the mechanism of solid state adhesion and welding in space simulated environment begun under Contract No. NAS1-2691, Task 5.

Contributing to this program was Mr. J. Roehrig. The principal investigator was Dr. M. J. Hordon. The technical monitor was Mr. J. Mugler, NASA-Langley.

INVESTIGATION OF THE ADHESION OF METALS IN ULTRA-HIGH VACUUM

By M.J. Hordon, J.R. Roehrig
NATIONAL RESEARCH CORPORATION

SUMMARY

Continuing a research study into adhesion, welding and friction behavior of selected metals in vacuum environments, measurements of the residual and frictional shearing forces generated during contact at vacuum levels below 1×10^{-9} torr were carried out for annealed copper, titanium and tungsten. Prior to contact under loads up to 1000 lbs, the mating cup-and-cone shaped surfaces were subjected to xenon ion gas bombardment or rotational self-abrasion to disrupt strongly adsorbed oxide films.

The results showed that the tendency for self-adhesion and friction was strongly dependent on the cleanliness of the contact surfaces and the mechanical strength of the metal. In particular, metals such as copper and tungsten with lower oxide bond energies showed a much greater tendency to adhere than titanium with a tenacious oxide difficult to remove. However, the ductile copper gave higher adhesion forces than the relatively harder tungsten. For equivalent loads, the self-adhesion and frictional shear forces decreased in the direction copper-tungsten-titanium at room temperature.

Adhesion-friction tests at temperatures up to 500°C showed that the effect of thermal softening and diffusion mechanisms was to increase the adhesion forces for copper and titanium while the comparative values for tungsten were largely unchanged. Increases in the adhesion shear force with an increase in the severity of abrasive loading were attributed to a proportionally greater disruption of surface oxides and a greater area of interfacial contact.

Generally, copper was found to weld readily at all temperatures. Titanium welded to some extent at temperatures above 275°C. Tungsten adhered to a small extent independent of the temperature level. The frictional forces followed similar directions.

INTRODUCTION

With the accumulated experience of many extended space probes under a wide variety of conditions, space scientists and materials designers have become aware that the adhesion of clean metallic surfaces may present a critical problem in the performance of flight components such as relays, camera shutters, antennae, bearings and other elements subjected to intermittent loading in vacuum environments. Metallic adhesion has frequently been suspected to be the cause of malfunctions in the orbital flight operation of equipment and test devices that functioned satisfactorily in the terrestrial atmosphere.

It has been reasonably established that solid state welding between metals in contact can occur provided surface metal ions are brought into atomic proximity (about 5 Angstroms).¹⁻⁴ At high temperatures, metallic atom bonding can occur by lattice diffusion mechanisms. At low temperatures, atomic contact requires the removal or disruption of inorganic or adsorbed surface layers. In addition, the formation of an area of contact large enough to cause macroscopic bonding generally requires plastic flow at the interface to relieve the elastic restoring forces generated under load and to flatten the microscopically irregular surface contours normally present in fabricated parts.

In the ultra-high vacuum of deep space, several mechanisms can act to remove the adsorbed films such as oxides normally present on metal surfaces. These include vacuum evaporation of boundary lubricant films, surface layer erosion by cosmic particle bombardment and mechanical abrasion by means of sliding or rotary contact under load. Thus it may be expected that metal components exposed to the space environment may eventually acquire film-free surfaces that are susceptible to cold welding even at temperature levels below the range of large scale diffusion bonding.

In this report the results of an investigation into several aspects of adhesion phenomena in ultra-high vacuums simulating the space environment are presented. Metallic bonding was studied for three materials including

copper, titanium and tungsten in the temperature range 20°C to 500°C under contact loads varying from 0 to 1000 lbs. An effort was made to simulate the service conditions expected in space exposure by subjecting the test surfaces to xenon ion gas bombardment and to rotary abrasion or sliding contact in order to disrupt contaminating films such as oxide layers.

The work covered in this report may be considered as a continuation of the initial studies of cold welding under simulated space conditions by National Research Corporation under NASA Contract NAS1-2691, Task 5. In that effort, major emphasis was given to a study of the gas ion bombardment technique for surface cleaning of adsorbed films at total pressure levels below 1×10^{-7} torr. In addition, changes in the electron work function of bombarded surfaces were determined by measurements of the potential variation of a retarded field diode in order to estimate the relative effectiveness of the bombardment dosage in removing contaminant films. In the current program, the experience and experimental data generated in the prior work was utilized for the ion beam bombardment tests.

In addition to measurements of the residual adhesion after removal of contact loads, determinations of the frictional properties of metal samples after ion bombardment or rotary self-abrasion for surface cleaning were also carried out at selected temperature levels. The object of the present investigation was to examine the adhesion-friction properties of materials as a function of mechanical strength, temperature, surface contamination and rotary or tangential sliding contact.

ADHESION APPARATUS

Vacuum Chamber

In the initial program of this series under NASA Contract NAS1-2691, Task 5, an ultra-high vacuum adhesion testing apparatus was constructed for studying rotational friction and cold welding under normal loading. This apparatus, with

several modifications, was used in the current work. The essential components of the system consist of a cylindrical vacuum chamber, a vertical loading mechanism capable of both rotary and vertical motion, an argon or xenon ion beam gun mounted integrally on the chamber wall together with the associated electrical and mechanical controls. Fig. 1 shows a view of the assembled apparatus with the ion beam gun mounted on the side of the chamber and the upper rotary drive loading support positioned above the chamber.

The test chamber was a 16 in. diameter stainless steel cylindrical vessel enclosed at both ends with seal plates supporting the loading stages. The plates were sealed to the vessel flanges by concentric "O"-rings. The flanges were refrigerated by cooling lines to about -37°C to minimize outgassing of the "O"-rings during thermal treatments. Optical and instrument ports were provided on the chamber wall including an 8 in. diameter port occupied by the ion bombardment gun. Resistance heating strips fastened to the vessel wall were used to radially heat the test chamber up to 400°C for thermal degassing.

The chamber pumping assembly consisted of a main 10 inch NRC diffusion pump in series with a 2 inch diffusion and mechanical back up pumps. The evacuation orifice of the test chamber was connected to the pumping units by a 10 in. diameter right angled duct provided with three internal liquid nitrogen cold traps as well as a modified chevron baffle liquid nitrogen trap. The "O"-ring flange seal between the duct and the baffle trap was refrigerated to prevent degassing of the seal. After a thermal degassing treatment, the system was capable of attaining a minimum pressure of 3×10^{-10} torr with the full experimental assembly. A schematic illustration of the vacuum system including the pumping units for the upper loading assembly is shown in Fig. 2.

Loading Mechanism

Vertical and rotary forces were imparted to the sample test surfaces by upper and lower loading assemblies. The lower loading system, schematically outlined in Fig. 3, comprised a force-transmitting shaft centrally aligned

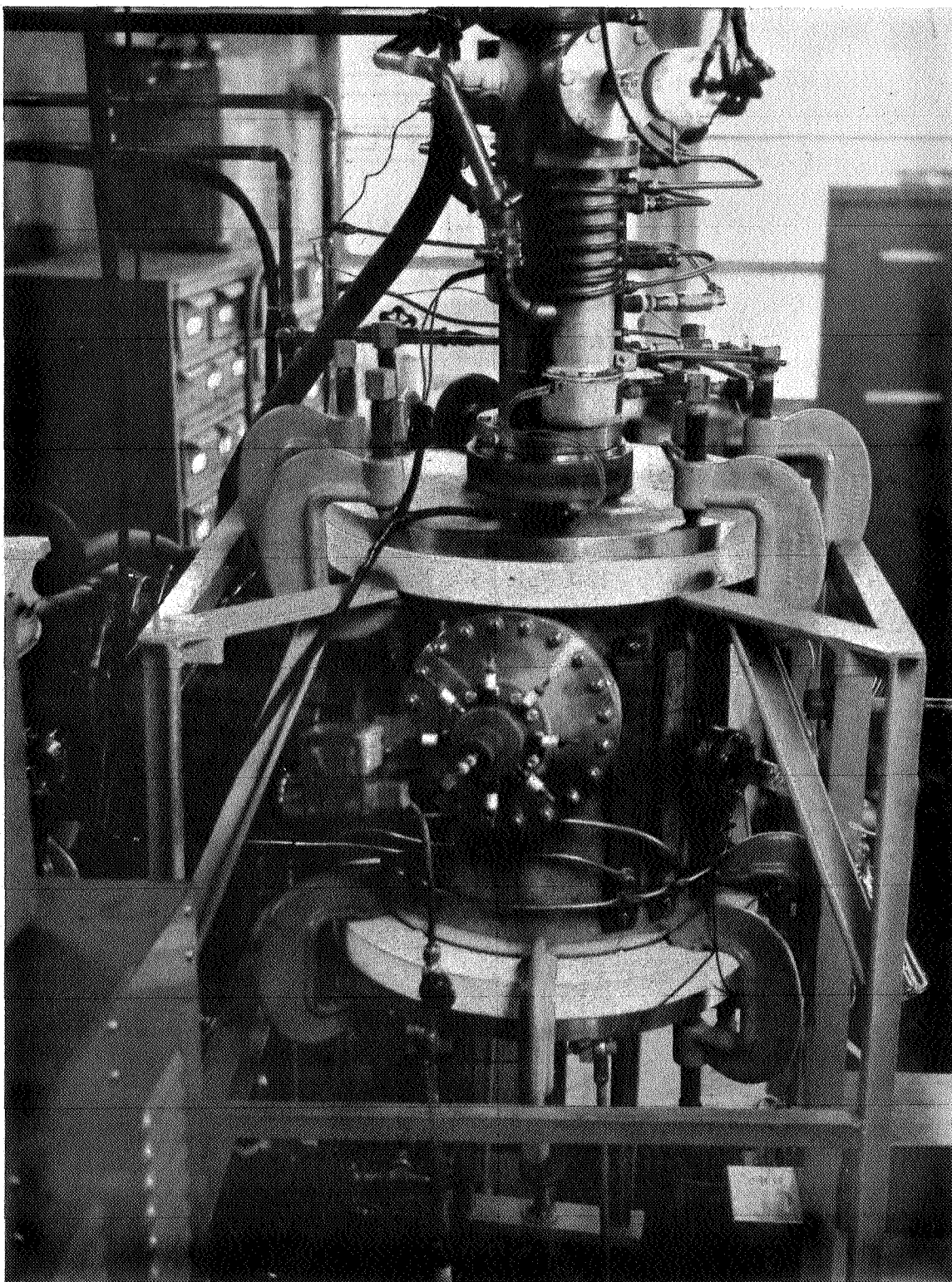


Fig. 1. Adhesion apparatus.

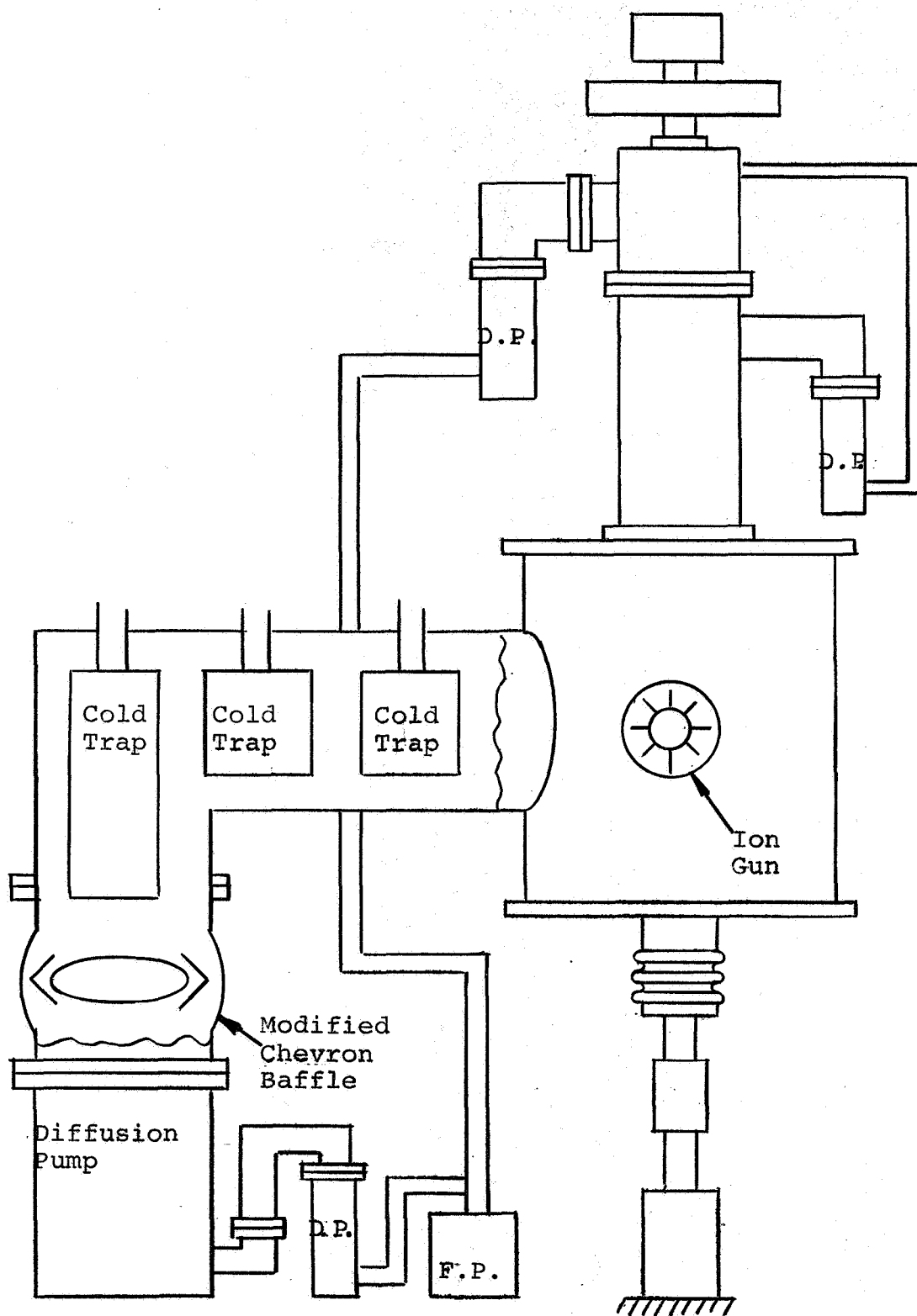


Fig. 2. Vacuum system for adhesion apparatus.

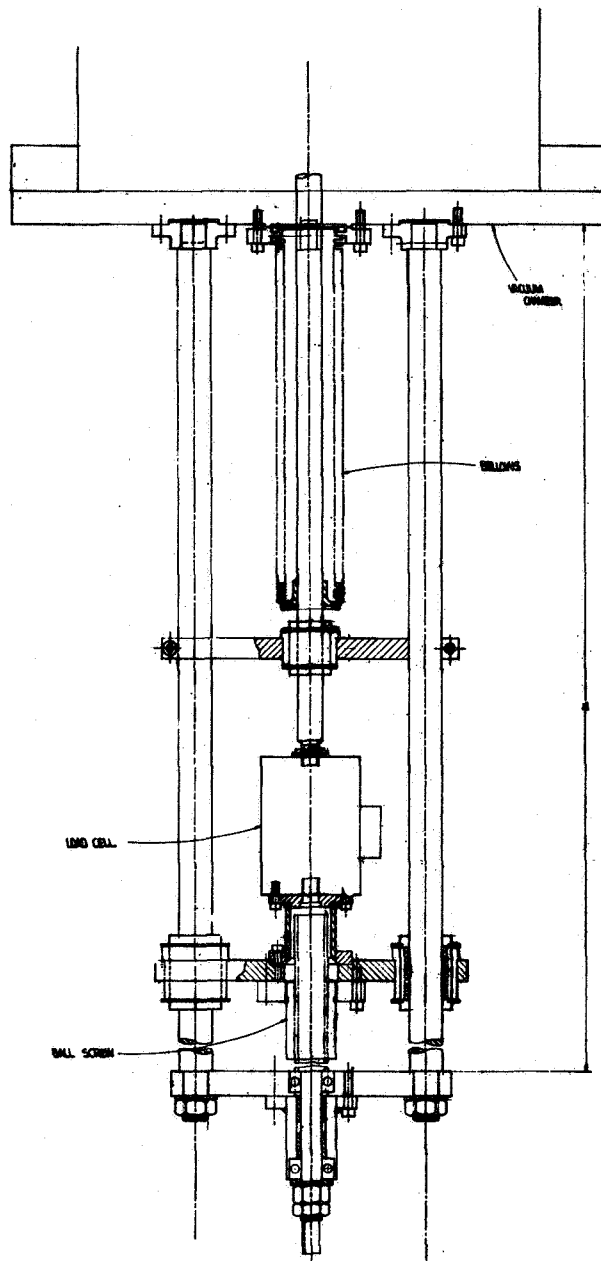


Fig. 3. Lower loading system.

by a steel compression cage assembly. The drive shaft contained a locking arrangement whereby either vertical or rotary motion could be achieved. In the vertical motion mode, a manual screw ram drive permitted shaft translation into the test chamber by means of a flexible bellows seal. The imposed force was monitored by a load cell directly attached to the shaft. The maximum ram force was 1000 lbs.

In the rotary motion mode, the shaft was uncoupled from the screw drive. A small chain drive powered by a 2 oz-in. torque sealed D.C. electric motor within the vacuum chamber was capable of rotating the shaft spindle at about 20 rpm under conditions of zero contact load.

The upper loading assembly, outlined in Fig. 4, comprised a rotatable shaft which vertically penetrated through a low conductance bearing seal in the upper flange plate into the test chamber. The shaft was enclosed in a cylindrical housing containing two liquid nitrogen cold traps and was separately evacuated by a 2 inch diffusion pump. The upper section of the shaft passed through a Teflon bearing seal into a guard vacuum enclosure and then continued through a double "O"-ring seal to the atmosphere.

The free end of the shaft was coupled to a 1/8 H.P. electric motor which could drive the shaft at about 20 rpm under compressive loads up to 100 lbs. With a 2 inch diffusion pump evacuating the guard vacuum enclosure to about 10^{-5} torr, a vacuum level of approximately 5×10^{-9} torr was obtained in the inner shaft housing. With this assembly, motor driven rotation of the shaft under normal loads up to 100 lbs. and manual rotation under loads up to 1000 lbs was obtained without adversely affecting the test chamber vacuum level.

The upper and lower loading shafts were rigidly aligned in the vacuum chamber by a sturdy guide fixture as illustrated in Fig. 5. Test specimens were positioned into fixed specimen holders attached to the loading shafts. As shown in Fig. 5, the loading stages were aligned so that the point of specimen surface contact coincided with the axis of the ion beam gun mounting.

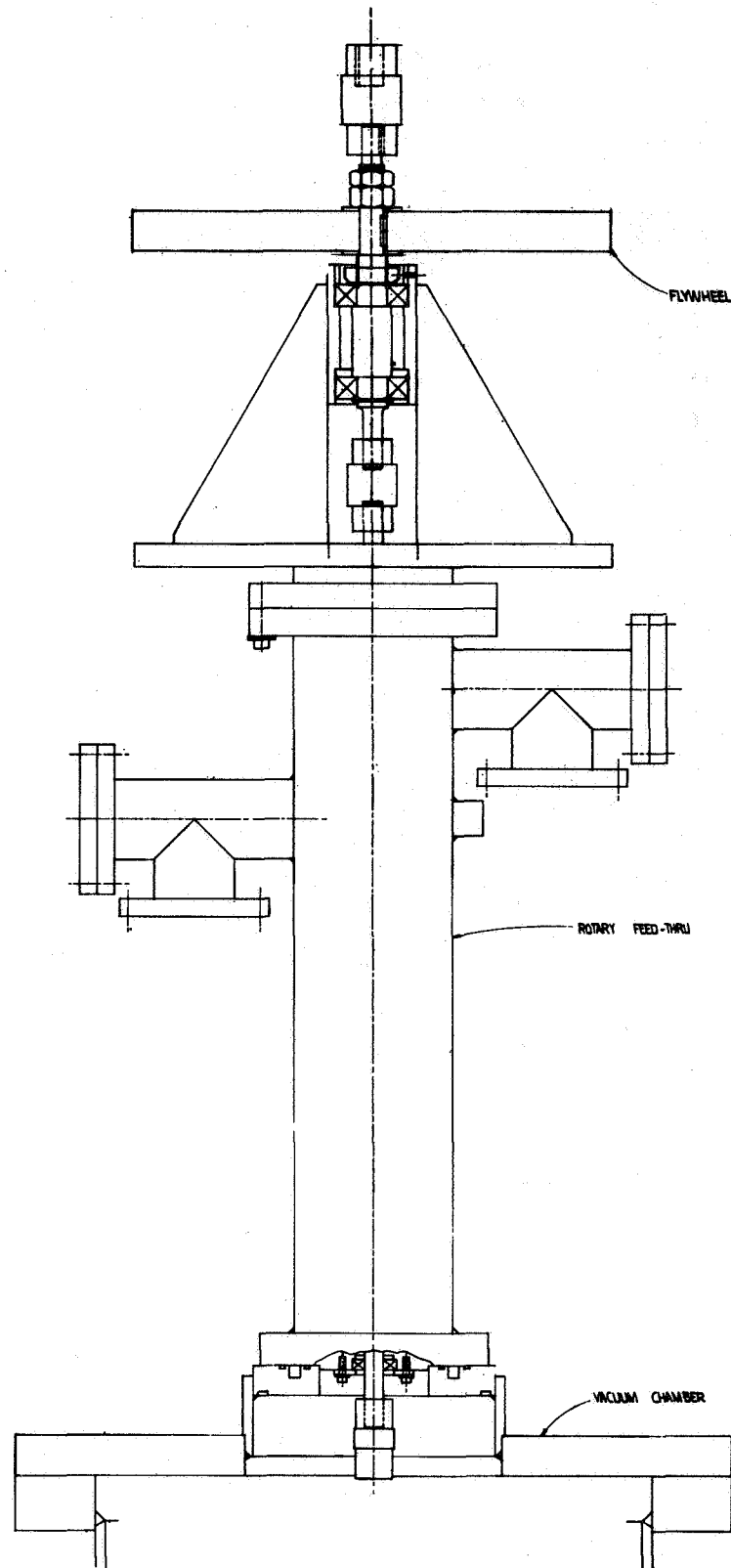


Fig. 4. Upper loading assembly.

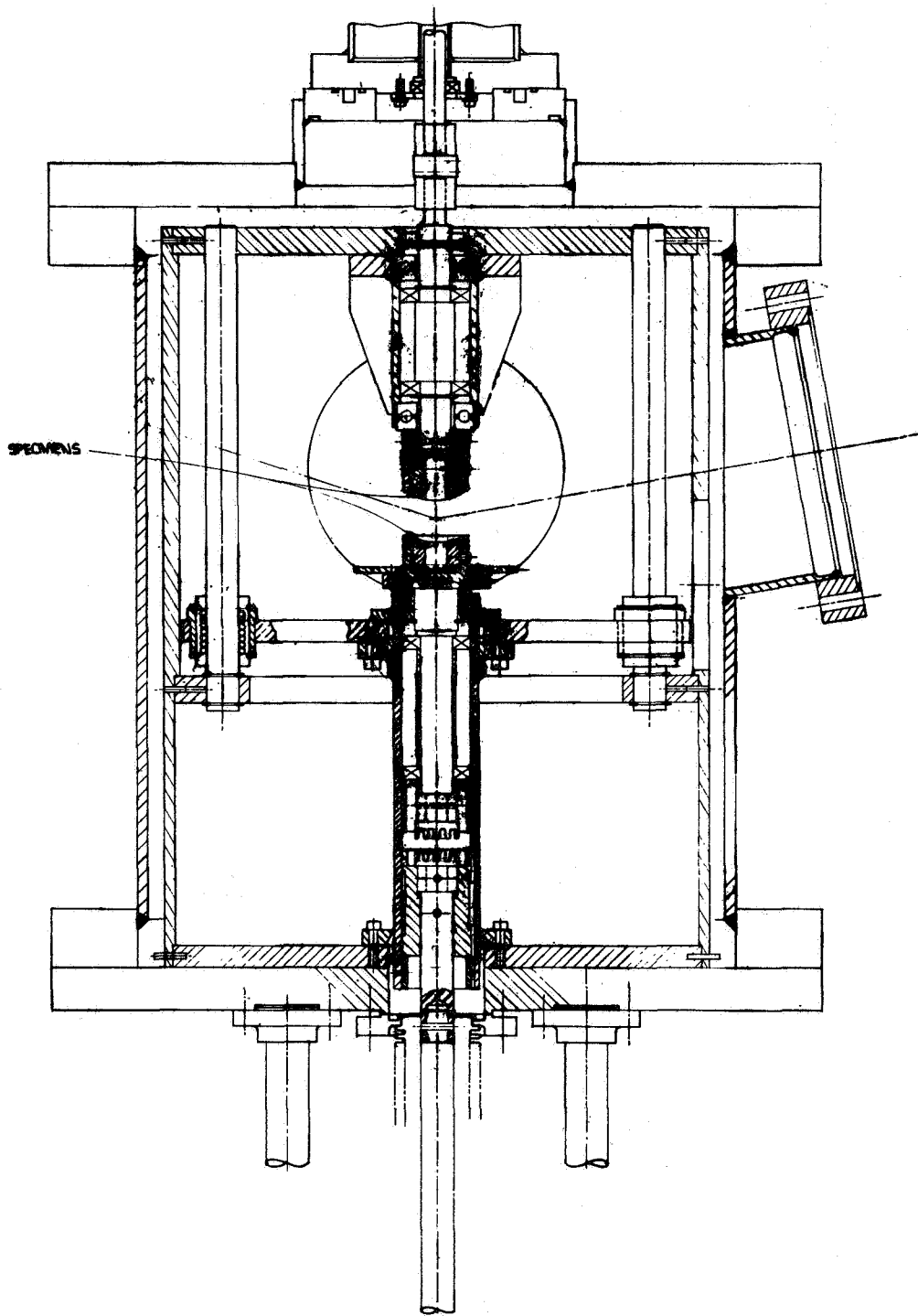


Fig. 5. Adhesion specimens mounting assembly.

Specimen Heating Unit

In order to conduct adhesion and friction tests at elevated temperatures, a split cylindrical, resistance wound furnace was devised to heat the specimen pairs. The furnace, illustrated in Fig. 6, consisted of a cylindrical stainless steel frame on which 30 mil platinum wire was longitudinally wound. The wire elements were isolated from the metal support by ceramic holders. The heating unit, about 1.5 in. in height and 2.75 in. in diameter, was constructed in two halves hinged together to permit convenient sample insertion. A stainless steel heat shield minimized radiation heating of the vacuum chamber. At the maximum power input of about 250 watts, specimen temperatures up to 600°C at pressure levels below 5×10^{-8} torr were recorded by chromel-alumel thermocouples embedded in the specimens.

Ion Beam Gun

The ion gun used for surface cleaning treatments was described in detail in the Final Report of the previous program in this series, Contract No. NAS1-2691, Task 5. Shown schematically in Fig. 7, the gun comprised an axially symmetric central tungsten cathode and cathode disc. Pure inert gases such as argon or xenon were bled into the discharge space at the tip of the central cathode. A^+ and Xe^+ ions were then extracted from the inner end of the discharge volume through a 95 pct transparent tungsten screen cathode. An axially symmetric magnetic field in the range 600-800 gauss was provided by disc-shaped magnets mounted outside the cathode housing which were removed during thermal degassing treatments. The ions were focussed into a beam after extraction by a cylindrical lens system. Electrostatic deflection plates at the lens exit were provided for beam deflection up to 5° to correct for alignment errors between the gun axis and the specimen surface target.

Designed as a low voltage discharge device to operate in vacuums less than 5×10^{-7} torr, the gun was usually operated at anode voltages in the range 1500-3000V. The resultant average ion energies measured at the target surface were generally in the range 800-1500eV.

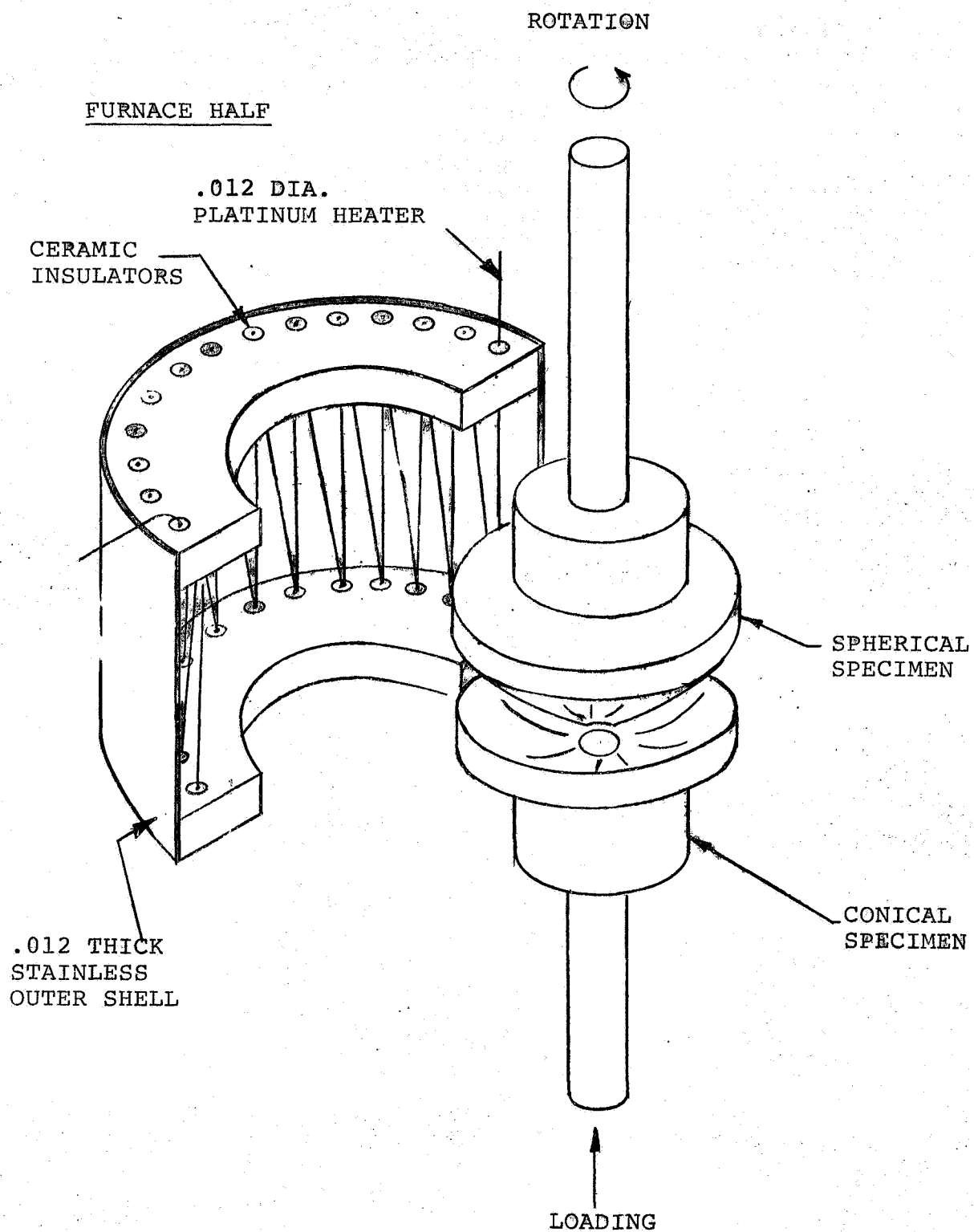


Fig. 6. Illustration of specimen heating unit.

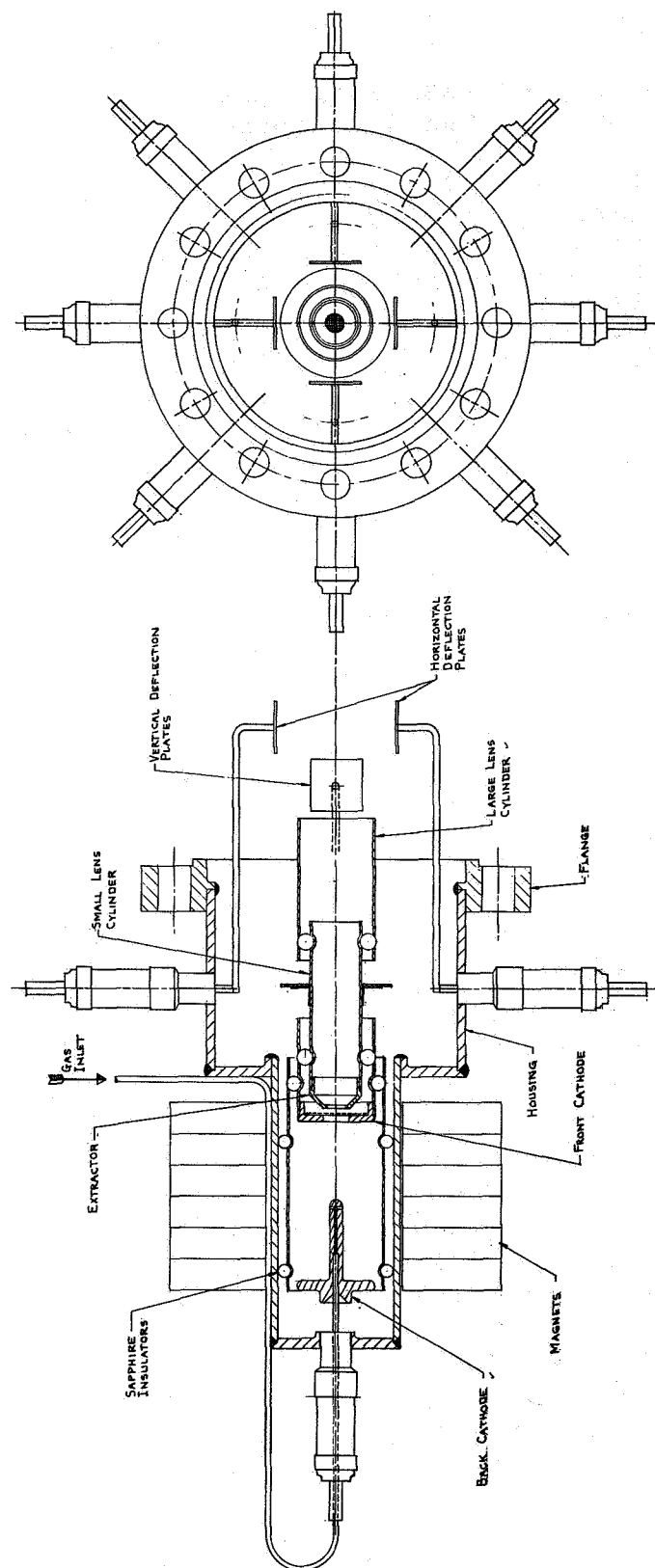


Fig. 7. Ion gun.

Specimen Design

Specimen couples similar in design to those fabricated in prior work were prepared of copper, titanium and tungsten. Fig. 8 shows the cup and cone surface geometry chosen to simulate space components in rotary bearing. The cup-shaped specimen designed for the lower loading stage was fabricated with the mating surface at a contact angle of 18.5° from the horizontal. This component was approximately $13/16$ in. in height and $1\ 3/8$ in. in diameter.

The cone-shaped component of the couple, about $1\ 1/2$ in. in diameter and 1 in. in height, was ground with a spherical mating surface with a radius of $13/16$ in. and was positioned in the upper loading stage. Both specimen types were machined with hollow axial cores 0.5 in. in diameter to facilitate fabrication. The cup angle and cone spherical radius were selected to enable the ion beam to bracket and cover both surfaces during bombardment. The ion beam axis was positioned to sweep both surfaces when the specimens were brought to a contact gap of about $1/4$ in. When under load, the area of contact was a narrow radial band.

EXPERIMENTAL TECHNIQUE

Specimen Preparation

Copper, titanium and tungsten specimens were carefully machined for installation in the loading stages. After fabrication, the tungsten specimens were stress relieved at 800°C for two hours and furnace cooled. Titanium specimens were annealed at 700°C for two hours. The copper specimens were stress relieved at 250°C for two hours. The resultant final hardness values taken from selected specimens is given in Table I.

After machining, the specimen test surfaces were ground and polished using standard metallographic procedures. The final diamond polish was carried out after heat treatment. The specimens were then ultrasonically cleaned in a detergent solution, followed by ultrasonic cleaning in acetone, alcohol and distilled water. After cleaning, the specimens were stored until use in a dessicator.

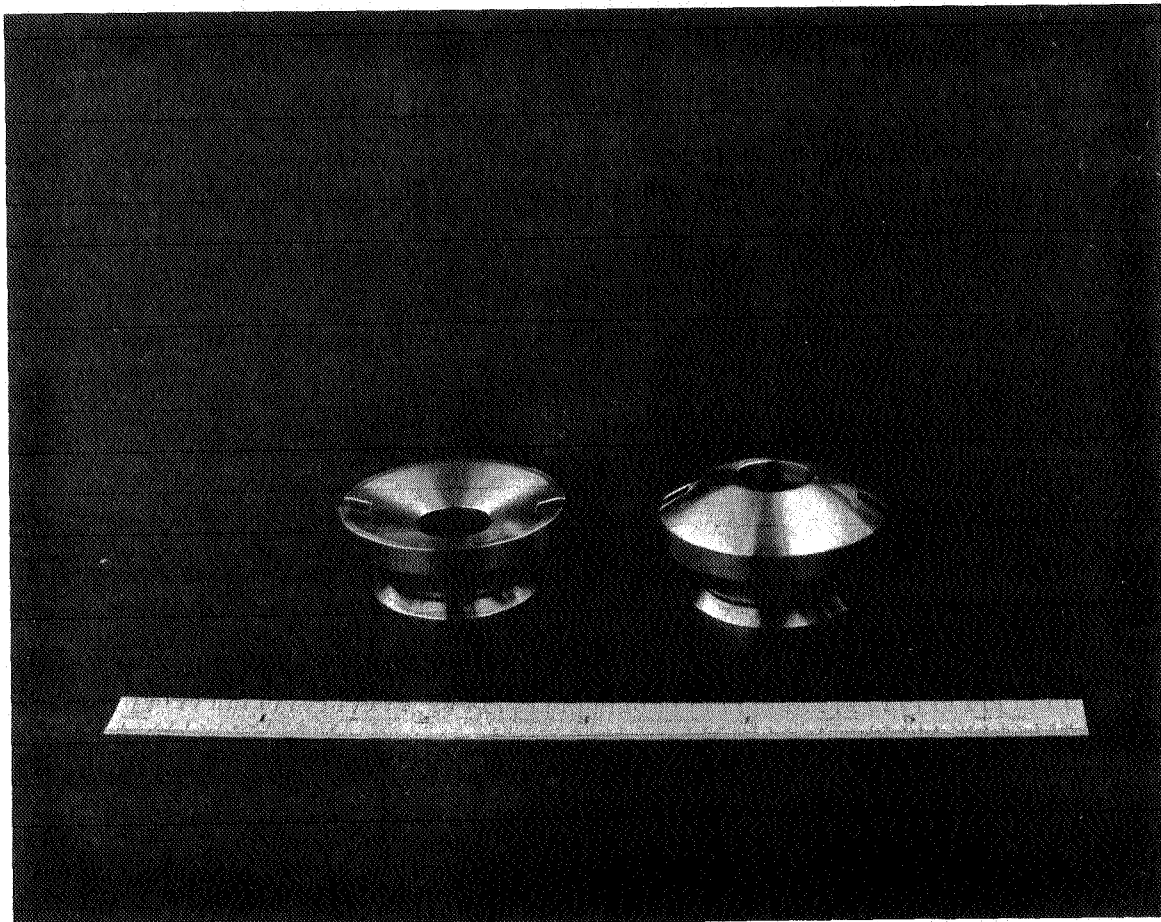


Fig. 8. Adhesion test specimen couple

Table I
Specimen Preparation Treatment

<u>Specimen Material</u>	<u>Heat Treatment</u>	<u>Hardness Rockwell A. Scale</u>
Copper	250°C, 2 hrs. air cool	27
Titanium	700°C, 2 hrs. furnace cool	21
Tungsten	800°C, 2 hrs. furnace cool	71.5

Vacuum Procedure

The vacuum system was assembled and thermally degassed at 350°C prior to installation of the specimens. Upon cooling, a system pressure of about 4×10^{-10} torr was recorded with the upper rotary drive chamber at about 5×10^{-9} torr. Operation of both upper and lower loading mechanisms did not degrade the vacuum. During the thermal treatment, the ion gun magnets were removed and the gun heated to about 350°C with an insulative thermal blanket.

With the system pressure established and all components tested, the chamber was filled with argon gas and the ion gun removed. The specimens were installed on the loading stages through the gun port which was provided with an expendible copper shear seal. Care was taken to ensure specimen surface cleanliness during this procedure. After installation, the ion gun was mounted on the port and the system was evacuated. The vacuum chamber was again subjected to a degassing treatment at 350°C for 10 hours including the intermediate nitrogen cold traps. Upon cooling the system, the ion gun was operated to heat the tungsten electrodes. The gun was maintained in operation at a minimal gas flow rate until the initially observed pressure rise disappeared.

Ion Bombardment

In preparation for the ion bombardment procedure, a copper collector plate about 1.6 cm^2 in surface area was initially positioned directly in the ion beam path immediately in front of the sample pair. The collector plate was used to monitor the ion emission current and to align the beam for maximum current flux. The plate was attached to the upper loading stage by a 20 mil nickel wire. When the ion beam had reached maximum current density and was stable, rotation of the loading stage ruptured the wire holder and dropped the plate out of the ion beam path thus permitting the specimens to be irradiated.

The ion gun was operated by bleeding argon or xenon gas through a Granville-Phillips leak valve into the gun discharge volume. The gas flow rate was limited to a level sufficient to maintain the system vacuum at about 5×10^{-7} torr. Previous experience with the gun characteristics had shown that this rate was adequate to produce ion current densities in the range $5 \times 10^{-7} - 10^{-9} \text{ amp/cm}^2$ with an applied anode voltage in the range 1500-3000V.

When the ion gun emission rate had been determined and the beam properly focussed and aligned on the specimen surface, the upper and lower loading stages were positioned so that the specimens had a $1/4$ in. gap between the contact surfaces. The stages were each continuously rotated at about 20 rpm to permit uniform sweeping of the surfaces by the impinging beam. Bombardment of the rotated samples was maintained for periods of 2 to 6 hours to ensure effective oxide film desorption.

Rotary Abrasion

In order to simulate possible service conditions in space, a procedure in which the upper convex-shaped specimen was rotated while in loaded contact with the lower cup-shaped specimen was devised. For this procedure, the lower stage rotary vacuum motor was removed and the lower stage spindle locked against rotary motion. Rotary abrasion was continued for periods up to 30 minutes with normal loads varying from 10 to 1000 lbs. For loads up to 100 lbs, the

upper spindle was motor driven at 10-20 rpm; for higher loads, the upper shaft was manually rotated at about the same speed.

For the adhesion test series at elevated temperatures, the vacuum furnace was installed after the specimens were positioned. To minimize thermal radiation emission to the chamber, the furnace was surrounded by a heat shield which precluded the use of ion bombardment surface cleaning. Hence, all the tests at temperatures above 20°C were conducted using the rotary abrasion method to disrupt surface films.

Test Procedure

For all three types of materials under investigation, standard testing procedures were used. For specimens initially surface cleaned by the ion bombardment method, the following test sequence was employed:

1. Starting with the sample pair at room temperature in a vacuum of approximately 5×10^{-10} torr, the samples were irradiated with xenon ions at current densities up to 5×10^{-7} amp/cm² for periods of 2 to 10 hours while in rotation to obtain uniform area coverage.
2. The samples were brought into contact with an elapsed time of about 6 sec while still under bombardment.
3. A standard test load of 1000 lbs was applied for five minutes followed by complete load removal. Upon release of the compressive force, the torque or shearing force required to rotate the upper hemispherical specimen relative to the lower stationary sample was determined by manual torque measurement.
4. After measurement at zero load, the standard 1000 lbs load was re-applied for the 5 min period. However, in successive tests, the compressive load was only partially released.
5. The frictional torque required for rotation was determined after each full loading sequence with 100, 200, 500 and 1000 lbs residual load.

6. During the test sequence, the compressive loads were measured by the load cell connected to the lower drive shaft, the rotational torques were measured by a torqueometer attached to the upper drive shaft and the system pressure was continuously monitored.

7. Upon completion of the test series, the specimens were optically examined.

For specimens subjected to the surface abrasion treatment, the following test sequence was used:

1. With the specimen couple at 20°C in an initial vacuum of about 5×10^{-10} torr, the specimens were brought into contact under loads varying from 10 to 500 lb. The upper specimen was then rotated relative to the fixed lower piece at 10-20 rpm for periods varying from 2-30 minutes.

2. Upon completing the rotational period, motion was stopped and the standard 1000 lb load was applied by increasing the abrasive load. The specimens were not separated after abrasion.

3. After 5 minutes load application, the compressive force was removed and the torque or shearing force required to separate the specimen couple was determined.

4. After measurement at zero load, the frictional torque under 100, 200, 500 and 1000 lbs residual load was measured after initially re-loading the specimens to the full 1000 lb force.

5. The compressive loads were monitored by a load cell on the lower drive shaft. The shear torques were measured by a torqueometer attached to the upper drive shaft.

6. Upon completion of the experimental tests, the specimens were optically examined for wear abrasion.

In several tests, particularly for copper, the test sequence was varied to permit the measurement of the tensile adhesion force in place of the zero load rotary shear force. The tensile or normal bonding force was determined after pinning both specimens by operating the lower drive shaft in reverse and observing the maximum cell deflection prior to rupture.

EXPERIMENTAL RESULTS

Ion Bombardment Tests

Measurements of the xenon ion beam current density with anode voltages varying from 2.0 to 3.5 kV were made prior to the adhesion tests using a collector plate with 1.6 cm² surface area. Current yields varying from 0.8 to 3.0 microamps were recorded during irradiation periods up to 5 hours with an average current density of about 1.0×10^{-6} amp/cm² at 3500 V. Assuming that the xenon ions produced in the discharge were singly charged, and noting that 10^{-6} amp = 6.25×10^{12} e/sec where e is the unit positive charge, the resultant average ion flux density was approximately 6.3×10^{12} Xe⁺/cm²-sec. Assuming that perhaps 1/100 of the ions recorded at the collector plate effectively reached the specimen surface areas, the estimated useful ion flux density was about 6×10^{10} Xe⁺/cm²-sec.

After calibration and alignment, specimen pairs of copper, titanium and tungsten were subjected to Xe⁺ ion dosages varying from 4×10^{14} to 1×10^{15} Xe⁺/cm². The anode voltage was maintained at about 3500V. The specimens were both rotated at 20 rpm during the irradiation period. With bombardment, the system pressure sharply increased from about 5×10^{-10} torr to about 5×10^{-7} torr. This pressure level was maintained by adjusting the xenon gas inflow.

At the close of the selected bombardment interval, the specimens were quickly brought together with an elapsed time of about 6 sec. The ion gun was shut down and the vacuum level was observed to decrease below 1×10^{-9} torr within 15 min. Upon contact, the specimens were brought under a compressive load of 1000 lbs for 5 min at room temperature. The load was then released and the shearing torque measured. Subsequently, the full load was re-applied for the same time increment and then partially unloaded to a residual compressive load of 100 lbs. The frictional shear torque was determined. The loading procedure was then repeated for successive residual loads of 200, 500 and 1000 lbs.

The results of the test sequences are given in Fig. 9. Residual adhesion forces were only detected for copper, an average value of about 10 in-lbs torque resulting from a bombardment dosage in excess of 6×10^{14} Xe^+/cm^2 and a compressive load of 1000 lbs. The frictional torques were generally observed to increase linearly with the initial normal loads. In the case of titanium, the variation of the frictional torque with applied load was linear throughout the range investigated. For copper and tungsten, however, the torque deviated from linearity above 100 lbs and 500 lbs, respectively, suggesting that work hardening or surface spalling was tending to lower the frictional resistance to rotation.

Rotary Abrasion Tests

Specimen pairs of copper, titanium and tungsten were tested in the standard procedure with the exception that prior to compression, the samples were self-abraded by rotating the upper component against the fixed lower sample under 10 to 25 lbs compressive force at room temperature. During the sliding and friction treatment, the system

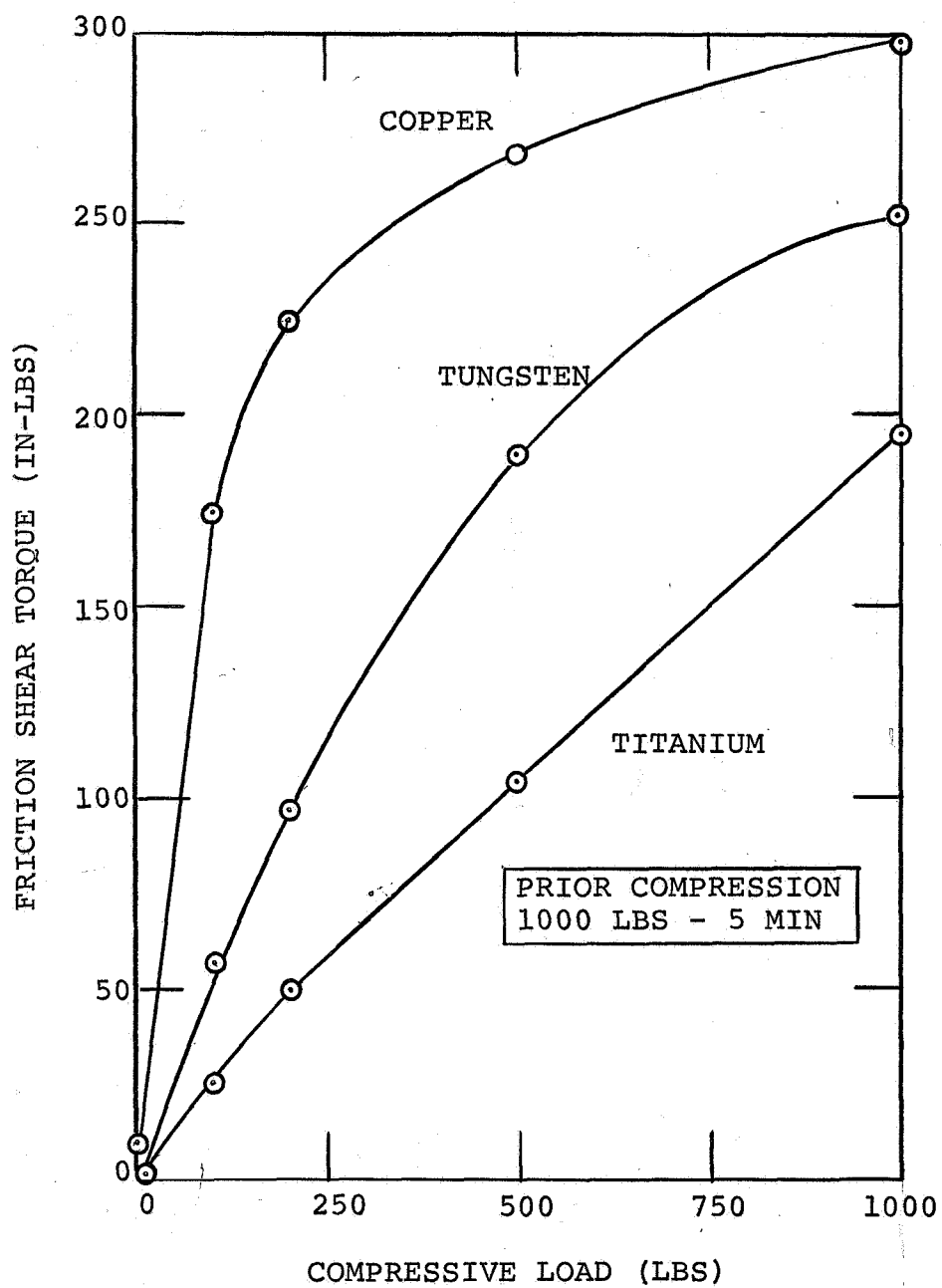


Fig. 9. Variation of the frictional shear torque with compressive load after Xe^+ ion bombardment.

pressure was observed to rise to about 2×10^{-9} torr. The abrasive treatment was continued for periods varying from 3 to 20 min at 20 rpm. Upon completion of the abrasion, rotation was stopped, the full compressive force was applied and the standard test sequence followed. During the compression period, the pressure was observed to decrease to $6-8 \times 10^{-10}$ torr.

The adhesion-friction results for this series of tests with the abrasive force and rotation time held constant at 25 lbs and 5 min respectively, are given in Fig. 10. It is evident that both copper and tungsten specimen couples showed evidence of residual adhesion under no compressive load with average values of 55 in-lbs and 30 in-lbs of torque, respectively. In comparison, the titanium couples failed to produce measurable bonding. As in the case of ion bombarded specimens, the frictional torques generally increased in linear proportion for all three materials at lower compressive loads. With contact loads above 500 lbs, both titanium and tungsten samples showed deviations from the linear relationship. In the case of copper, the torque values above 200 lbs residual load were beyond the limit of torque measurement, 300 in-lbs.

The effect of the abrasion force on the adhesion-friction values generated in vacuum was examined for the three types of materials in the range 25 to 500 lbs. The rotational time and angular velocity was held constant at 3 min and 10 rpm. The results for titanium are shown in Fig. 11. At zero residual load, no welding or resistance to rotary shear was observed below an abrasive force of 300 lbs. Under residual loads up to 1000 lbs., after an initial compression and partial release, frictional torques initially showed a rapid increase with abrasive contact forces up to 150 lbs. With further increase in the abrasive load, the rate of increase in the shear torque was noticeably slowed.

Generally similar results were obtained for tungsten as shown in Fig. 12. In this case, the rate of increase in the frictional torque with abrasion load was markedly lower than for titanium or copper. The residual resistance to shear at zero load increased from 30 to 40 in-lbs with an increase in the contact load during abrasion from 25 to 500 lbs. For a constant residual load of 1000 lbs, the

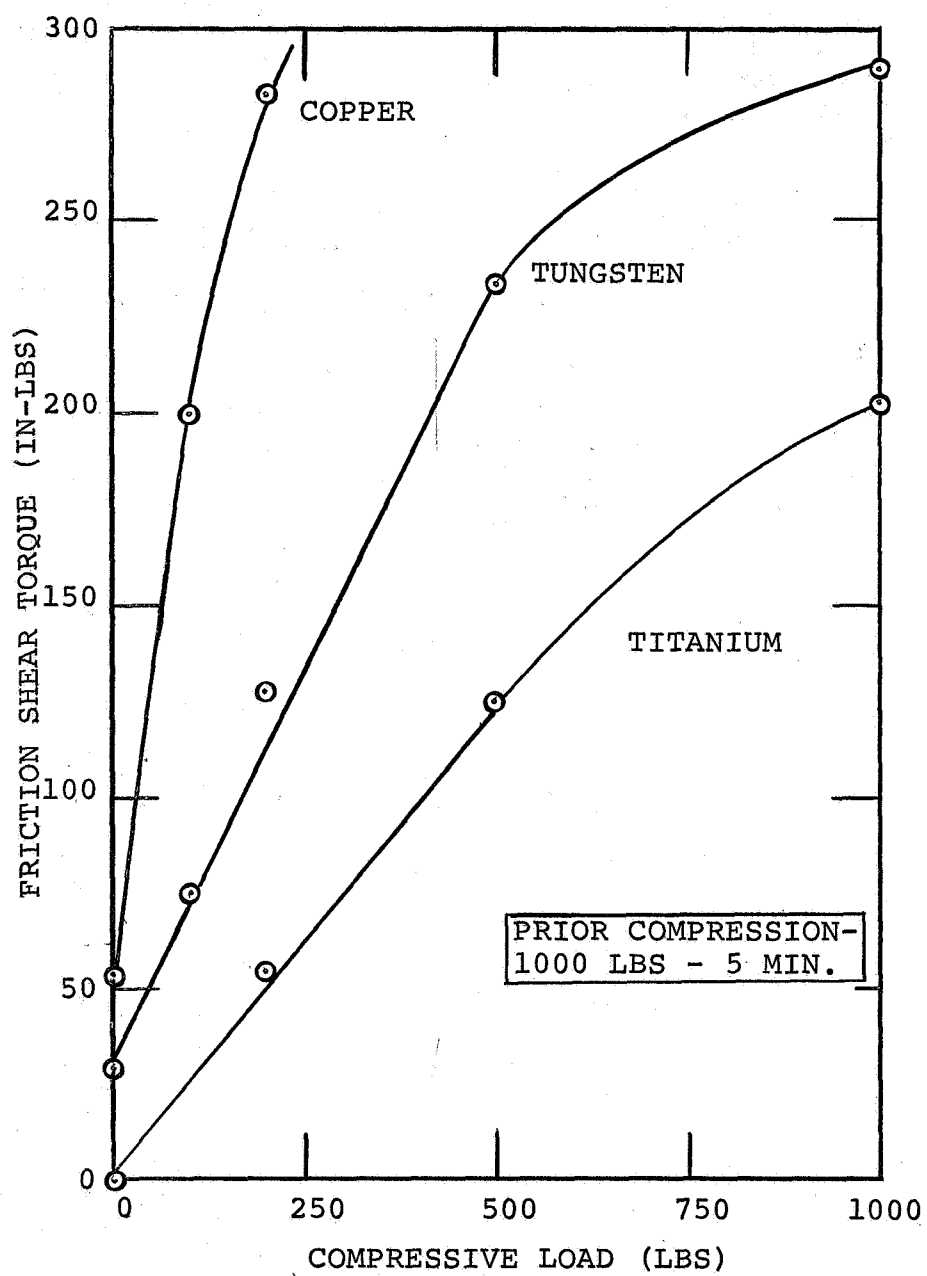


Fig. 10. Variation of the frictional shear torque with compressive load after rotary self-abrasion.

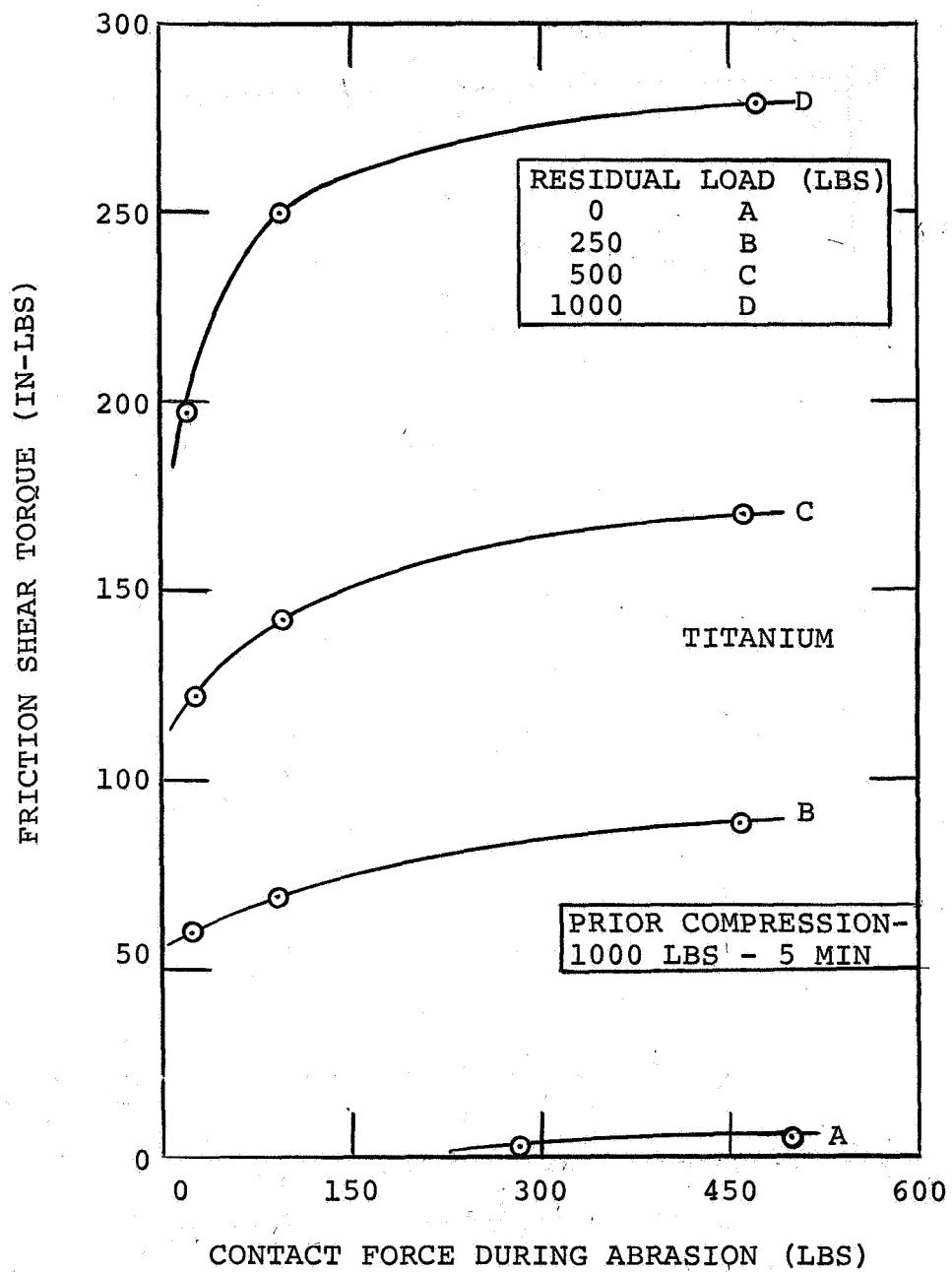


Fig. 11. Variation of the rotational shear torque with abrasive load for titanium.

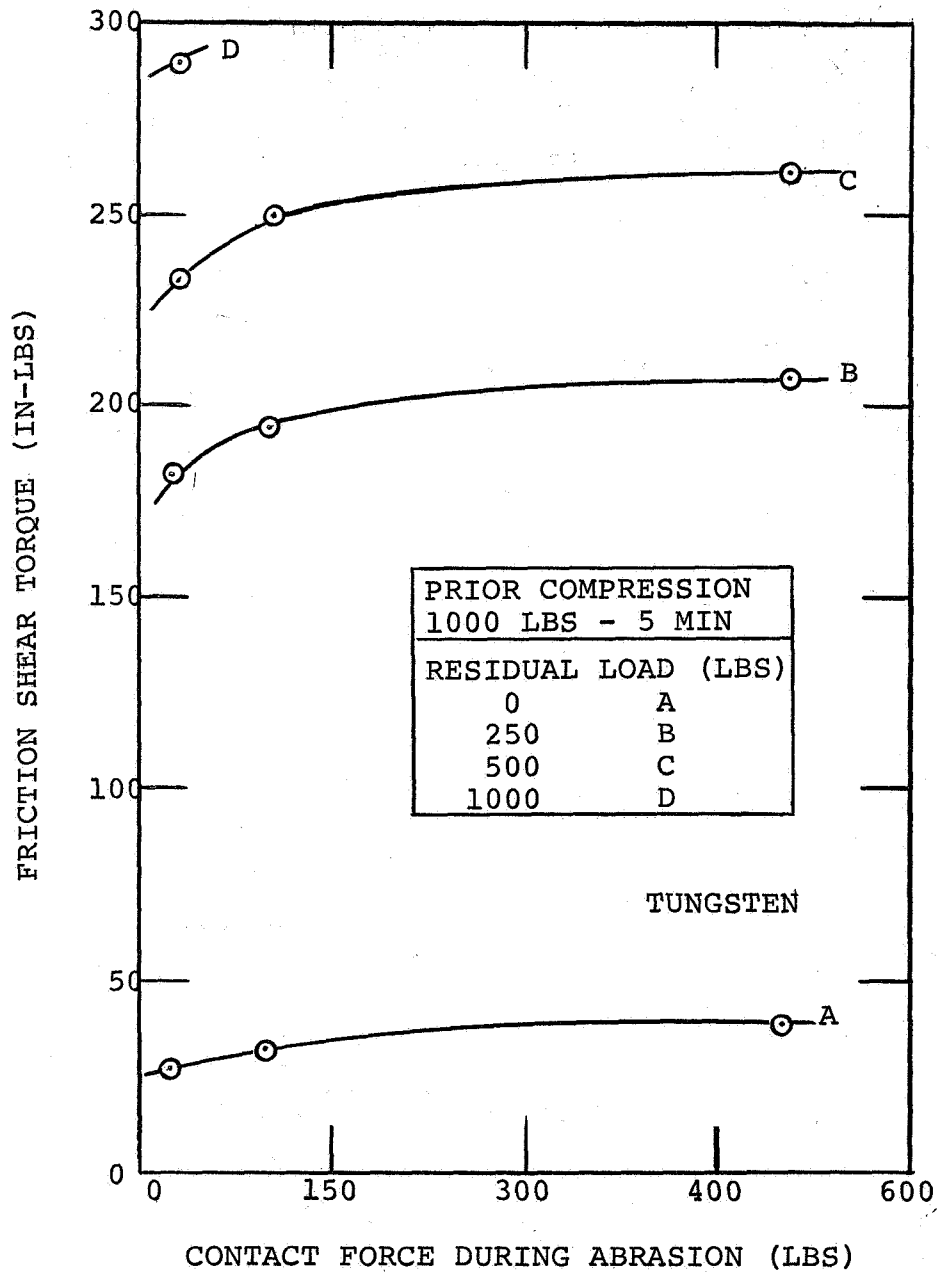


Fig. 12. Variation of the rotational shear torque with abrasive load for tungsten.

measured shear torques exceeded 300 in-lbs for abrasive forces greater than about 75 lbs.

For copper, the tests showed that this material was extremely sensitive to the abrasion force level as shown in Fig. 13. For this relatively soft metal, an increase in the abrasion force from 25 to 500 lbs resulted in an increase in the zero load shear resistance from 55 to 120 in-lbs, indicating a substantial gain in the welding force. Increases in the residual load above 100 lbs after initial deformation at 1000 lbs exceeded the limits of measurement for the system.

In the particular case of copper, measurements of the normal separation or rupture forces were also undertaken with equivalent abrasive and loading test sequences in order to correlate the residual adhesion forces with direct measurements of the residual shear torque. With copper specimens subjected to rotary self abrasion under 25 to 500 lbs for 3 min at 10 rpm and tested with a full 1000 lbs contact load, normal rupture forces in the range 30 to 65 lbs were obtained as shown in Fig. 13. Comparison of the torque and tensile force values showed that a shear torque of 50 in-lbs could be approximately equated to a rupture force of 30 lbs for copper.

Residual Adhesion Tests at Elevated Temperatures

A series of adhesion tests were conducted at elevated temperatures up to 500°C using the rotary abrasion method to strip surface oxides from the specimens. At selected temperature levels, the abrasion time and loading level were varied to determine the optimum parameters for abrasive cleaning.

The effect of temperature on the zero load residual bonding torque after abrasive action for all three metals is shown in Fig. 14. It is evident that adhesional forces for both copper and titanium were sensitive to temperature. However, the residual shear torque for tungsten did not change appreciably in the temperature range investigated.

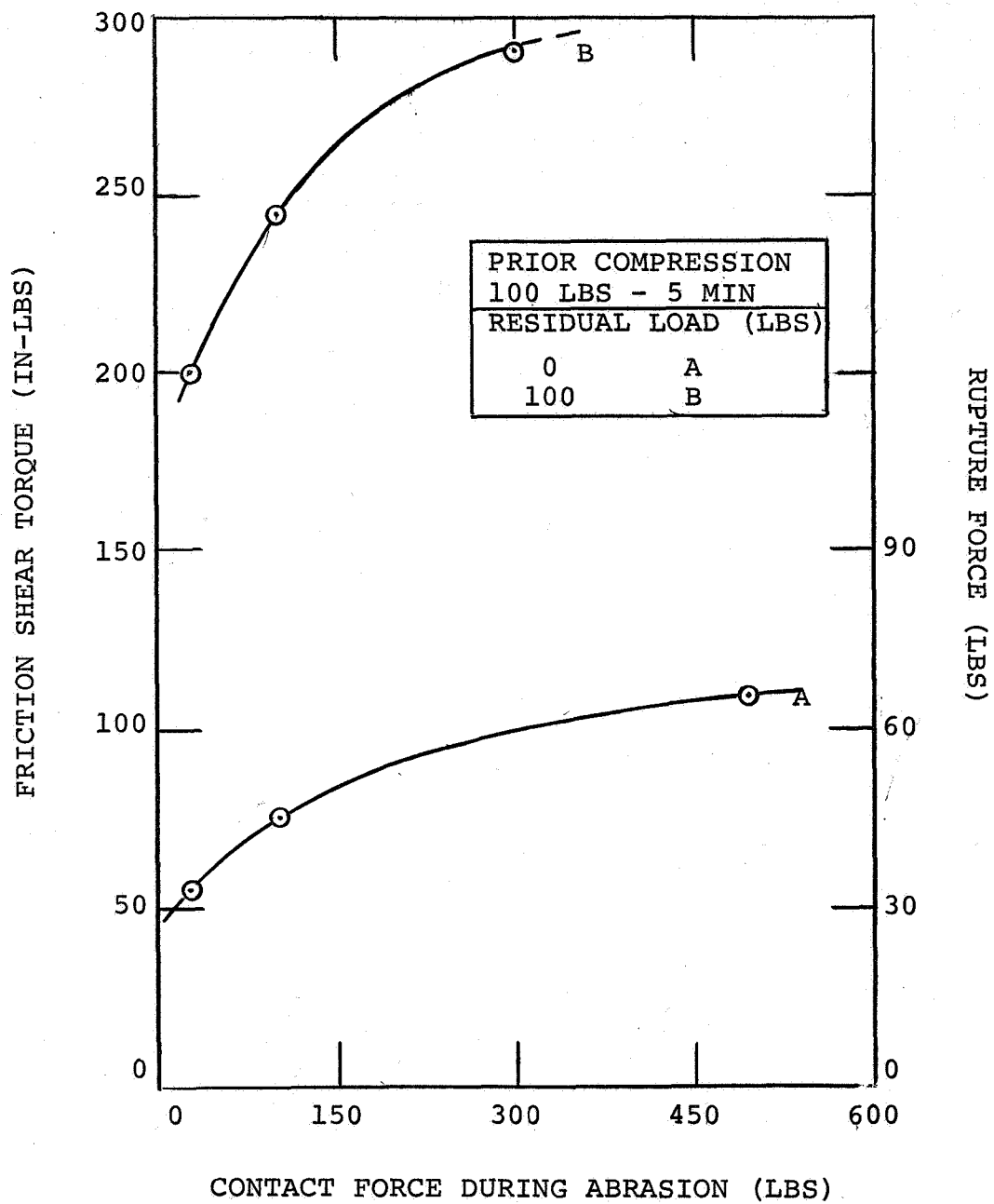


Fig. 13. Variation of the rotational shear torque with abrasive load for copper.

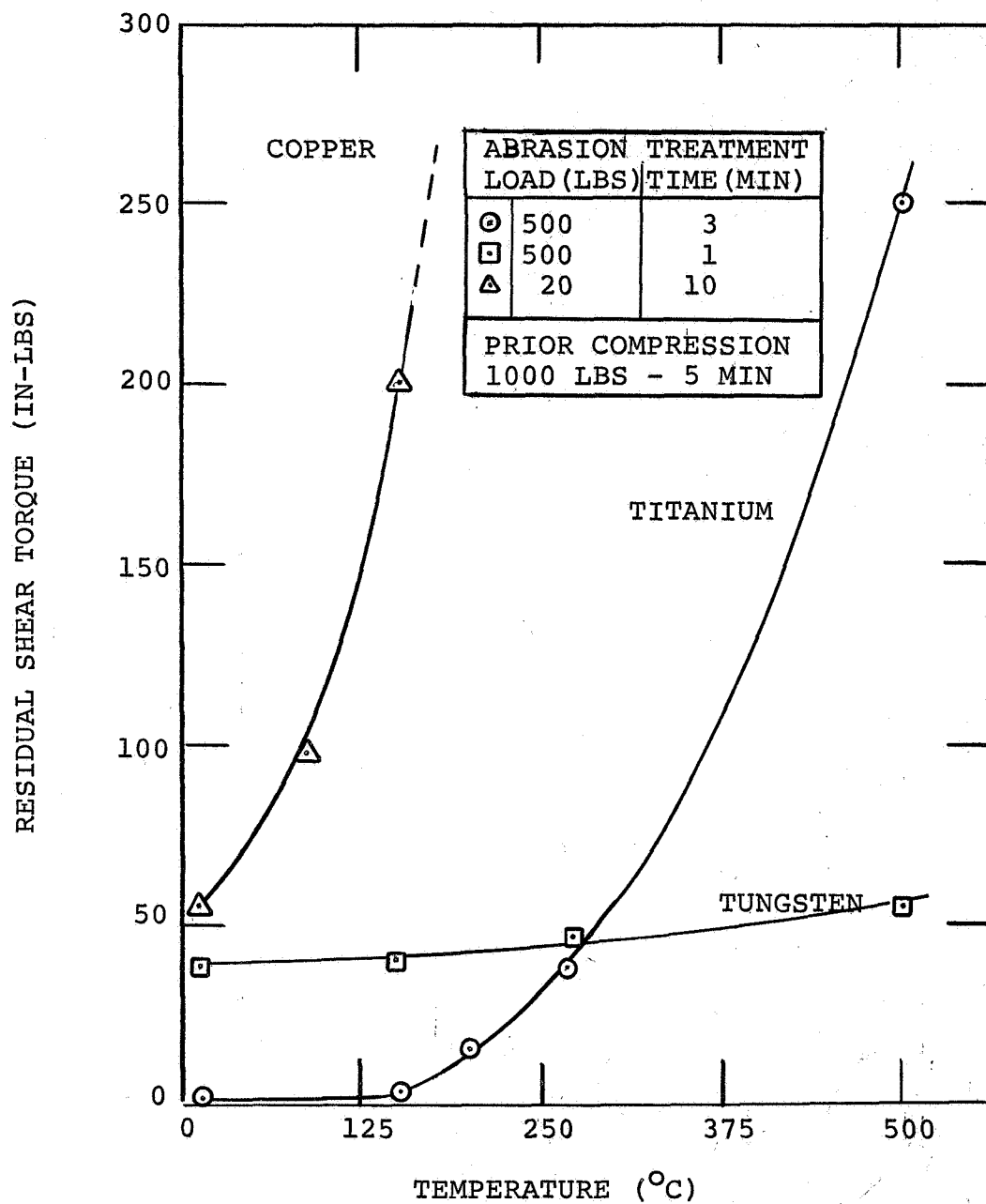


Fig. 14. Temperature dependence of the residual adhesion force after rotary abrasion.

The data show that adhesion bonding in titanium was largely negligible below 150°C. With further increase in temperature, the adhesion shear force increased substantially, however, reaching about 250 in-lbs at 500°C. For copper, the adhesion force exceeded the limit of measurement at temperatures above approximately 200°C.

The dependence of the adhesion shear force on the severity of the abrasion treatment is illustrated in Fig. 15 in which the shear dependence on the abrasive load at a constant time of 3 min and for several temperature levels is given. For copper and titanium, the increase in the shear torque with abrasive load was generally linear; tungsten, however, showed a flatter response indicating that the abrasive load was of secondary importance in determining the amount of bonding force.

At selected temperature and abrasive force levels, measurements of the effect of abrasive time at constant load on the adhesion force at zero load were carried out. Representative results are shown in Fig. 16 for the shear torque dependence on abrasion time at constant contact loads at 500°C. It was apparent that an increase in the period of abrasion up to about 10 minutes resulted in a significant gain in the residual shear torque for both tungsten and titanium. For abrasion times greater than 10 min, the rate of increase in the adhesion torque dropped substantially, suggesting that the self-abrasion technique accomplished the major portion of the contact surface cleaning in the initial 10 minutes. After the initial abrasion period up to 10 min, it was more effective to increase the abrasive load than to increase the abrasion time at constant load.

Shear Friction Tests at Elevated Temperatures

Rotary frictional tests were conducted at selected temperature levels with normal compressive forces ranging from 100 to 1000 lbs. The frictional force was determined as the shear torque required for rotation under load. Frictional test sequences were performed after abrasive cleaning. The results for titanium and tungsten specimens

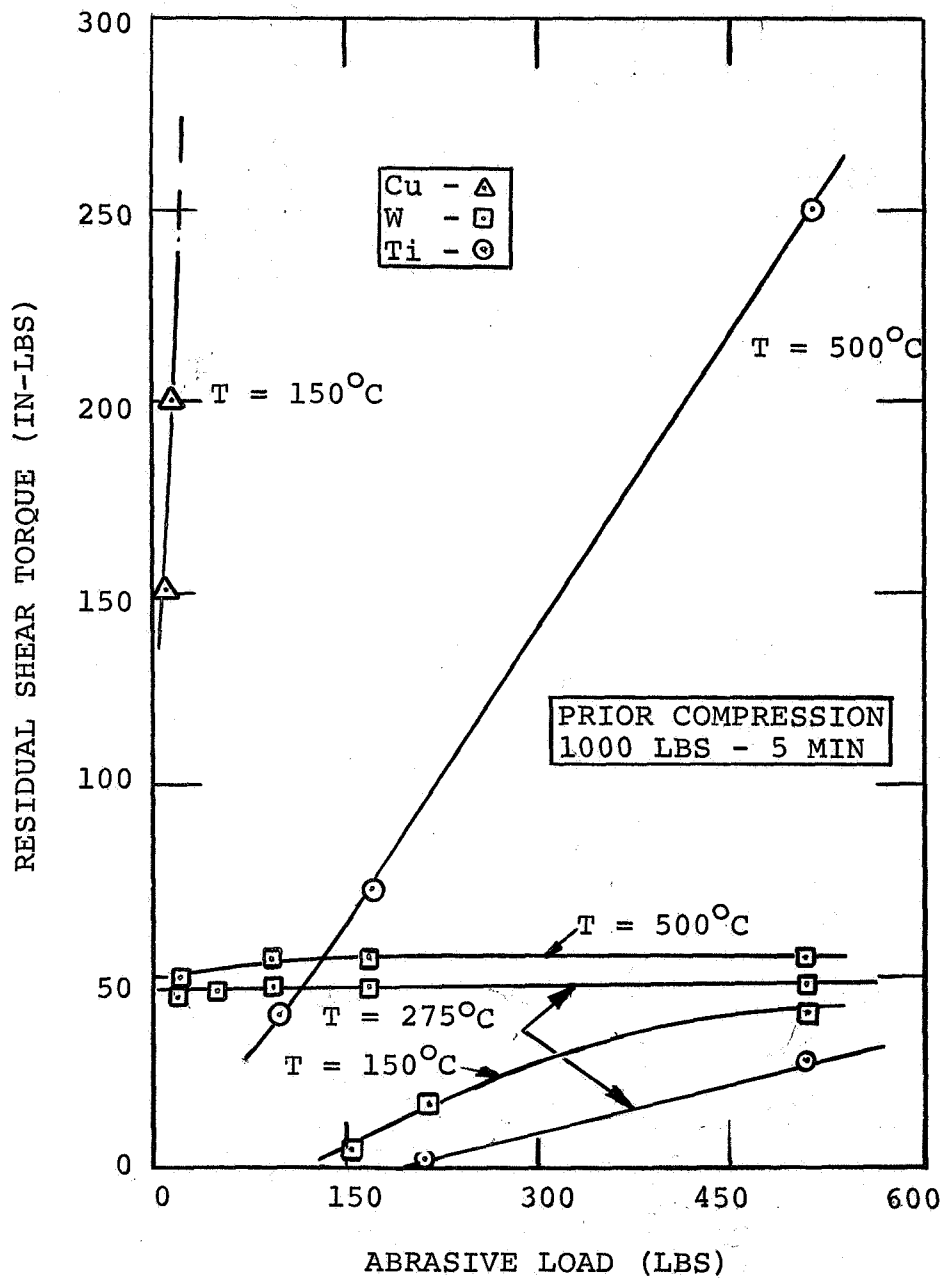


Fig. 15. Dependence of the residual shear torque on abrasive load at constant time for selected temperature levels.

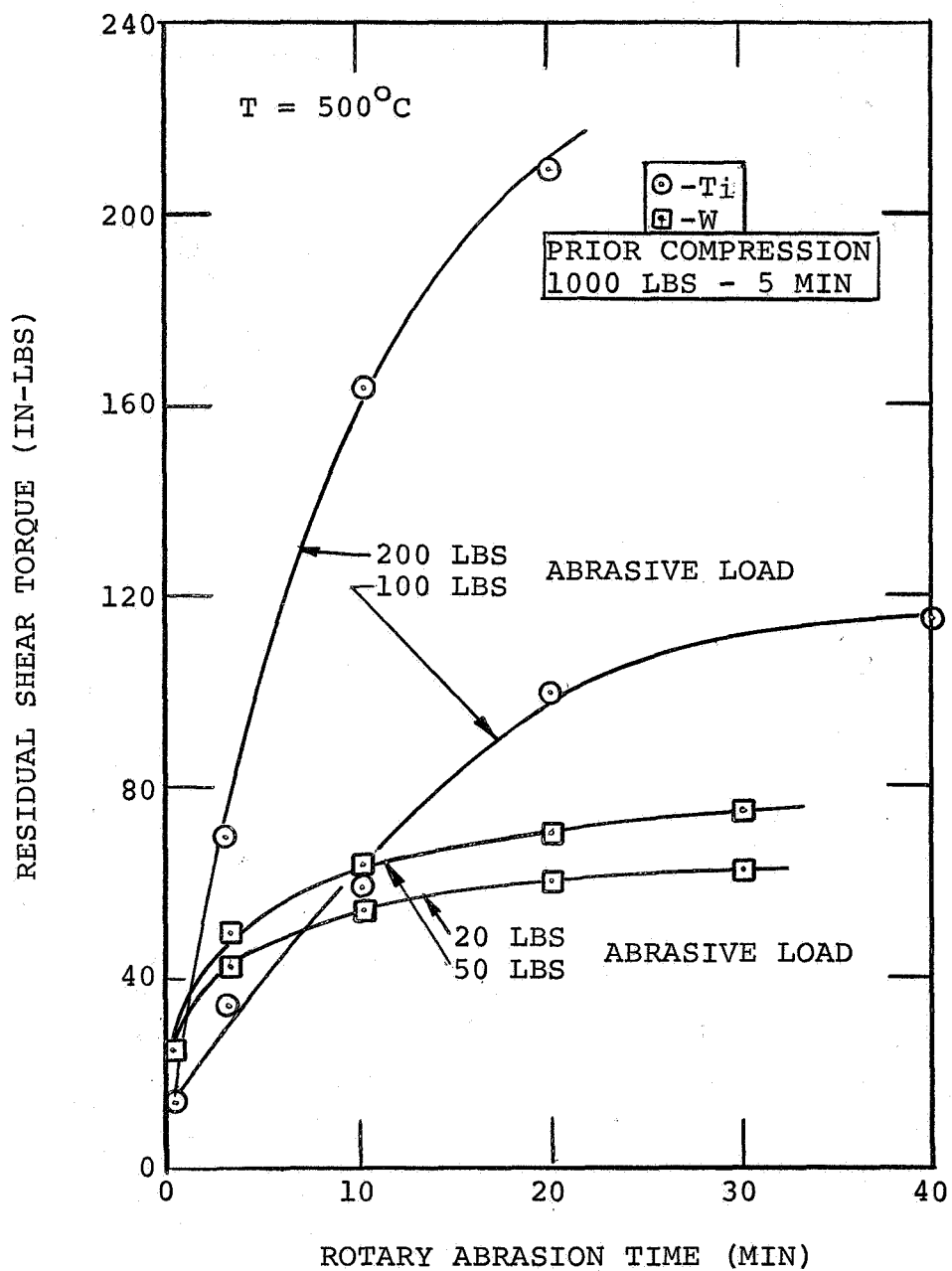


Fig. 16. Increase in residual shear torque with abrasion time at 500°C at selected abrasive loads.

are given in Figs. 17 and 18, respectively, and include the frictional data taken at room temperature for comparison. It is evident that the friction torque decreased with rise in the test temperature for both metals. At the higher temperature and lower load levels, the friction torque generally varied linearly with the applied compressive load. However, at the higher load and lower temperature levels, the frictional shear torque departed from linearity and showed a lower rate of increase with applied load.

In tests on copper at elevated temperatures, the material was found to soften appreciably, raising the friction torques above the limit of measurement.

The shear torque may be converted to a maximum shear stress τ acting in the contact zone according to the expression:

$$\tau = \frac{16H}{\pi d_o^3 [1 - (d_i/d_o)^4]} \quad (1)$$

where H is the torque, d_i and d_o are the inner and outer diameters of the circular contact zone, respectively. Since the band width of the contact zone is generally narrow, the maximum outer fiber stress may be assumed as the average shear stress over the deformation band. Values of d_i , d_o and H for various temperature levels are given in Table II.

The ratio of the shear stress τ to the normal compressive stress σ_N may be taken as an indication of the friction coefficient f for the vacuum conditions in the present work. The friction coefficient will then be:

$$f = \frac{\tau}{N/A_c} \quad (2)$$

where N is the compressive load taken constant at 1000 lbs and A_c is the area of the contact zone. Values of A_c and f are also given in Table II for tungsten and titanium.

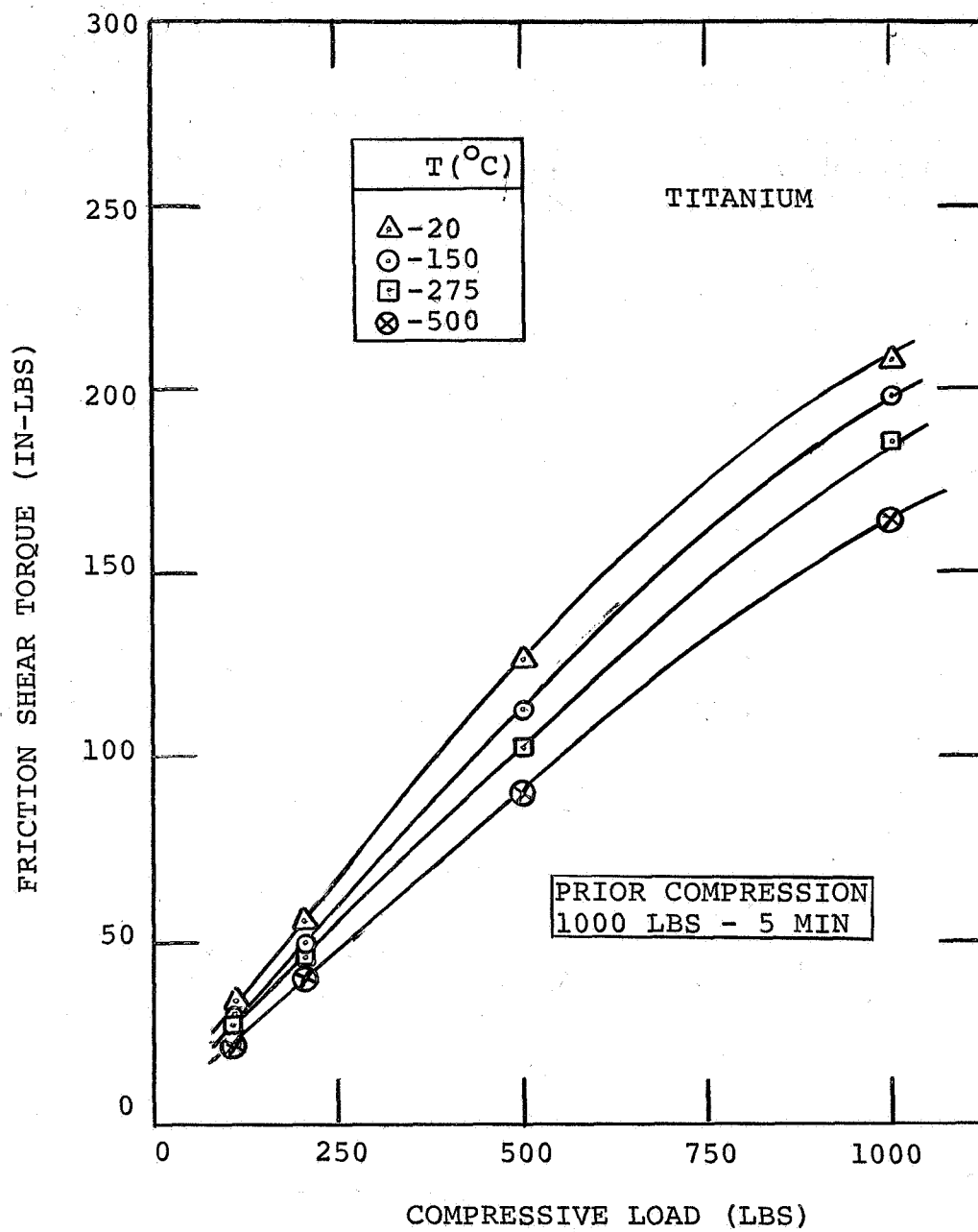


Fig. 17. Temperature dependence of the frictional torque with compressive load after rotational abrasion for titanium.

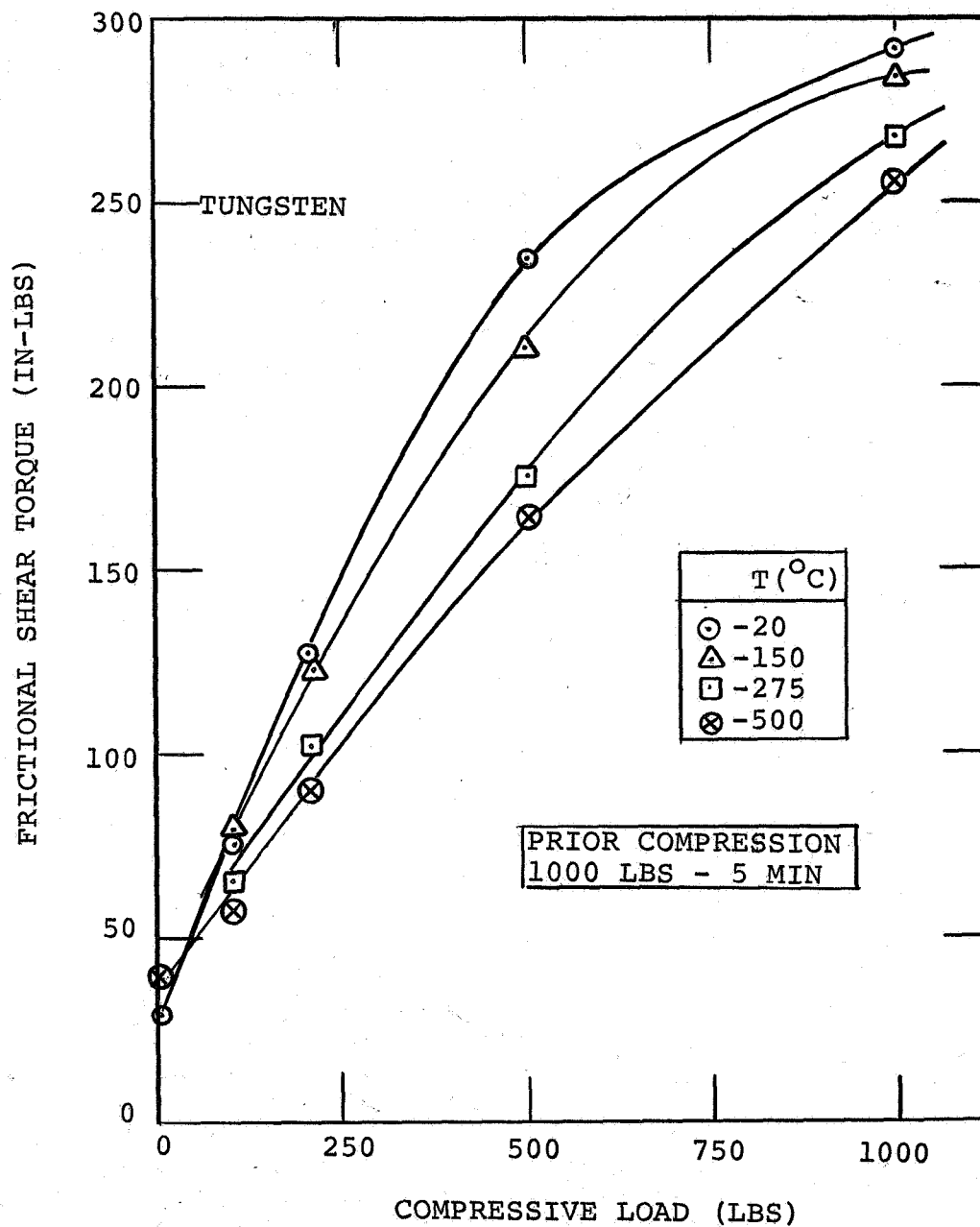


Fig. 18. Temperature dependence of the frictional torque with compressive load after rotational abrasion for tungsten.

It is apparent that tungsten, after self-abrasion, offered greater resistance to rotational sliding than titanium. The friction coefficients of both metals were observed to decrease slightly with temperature, the effect of temperature being more noticeable with W than with Ti.

Table II
Temperature Variation of Vacuum Friction Parameters

<u>Temp.</u> (°C)	<u>d_i</u> (in.)	<u>d_o</u> (in.)	<u>H</u> (in-lbs)	<u>τ</u> (psi)	<u>A_c</u> (in ²)	<u>f</u>
<u>Tungsten</u>						
20	0.724	0.755	290	22,400	0.036	0.80
150	0.711	0.796	285	7,840	0.099	0.78
275	0.685	0.834	268	4,300	0.178	0.76
500	0.652	0.870	257	3,080	0.262	0.74
<u>Titanium</u>						
20	0.718	0.748	213	16,700	0.034	0.58
150	0.696	0.808	203	4,380	0.129	0.57
275	0.677	0.848	192	2,640	0.209	0.57
500	0.641	0.892	170	1,625	0.303	0.55

Diffusion Bonding at Elevated Temperatures

Since materials such as copper and titanium showed a substantial temperature dependence for parameters such as residual adhesion bonding and abrasive load during rotation, it was considered instructive to examine the influence of diffusion bonding on the measured adhesion properties. Accordingly, time-temperature tests were carried out after abrasive cleaning in which the usual 1000 lbs load compression step was altered to vary the time under load from the standard period of 5 min to approximately 100 min at temperature. After the holding

period, the load was released and the residual shear torque determined.

Representative results are presented in Fig. 19 which shows the variation of the residual shear torque with contact time under the full compressive load. It is apparent that the contribution of a diffusional process to the welding bond was negligible in tungsten, appreciable in titanium at 500°C, and extremely important for copper above 275°C. Measurements taken at different temperature levels, as shown for tungsten and copper, showed that increases in temperature produced larger changes in the residual adhesion torque than increases in contact time, in general agreement with diffusion-controlled processes.

DISCUSSION

Ion Bombardment Experiments

The adhesion or residual shear torque results obtained after prolonged Xe^+ ion bombardment showed that of the three metals under study, only copper gave evidence of welding at room temperature. In related studies, it has been established that softer materials which flow relatively easily under loads exceeding the compressive yield strength will produce large macroscopic adhesion forces. High strength materials, on the other hand, which have a large elastic strain component, will recover the deformation upon release of load and rupture localized welded areas.

Aside from the plastic strain requirement, it is of interest to estimate the efficiency of the ion bombardment method in stripping off surface atoms to permit metal-to-metal atomic contact necessary for metallic bonding. In the present work, ion dosages of $0.4 - 1.0 \times 10^{15} \text{ Xe}^+/\text{cm}^2$ over a period of 2 to 5 hours were employed to sputter the specimen surface layers with an estimated median energy of 800-1500eV, well above the usually accepted threshold values of 25-50eV needed to disrupt surface atomic bonds.⁵ Considering the bombardment

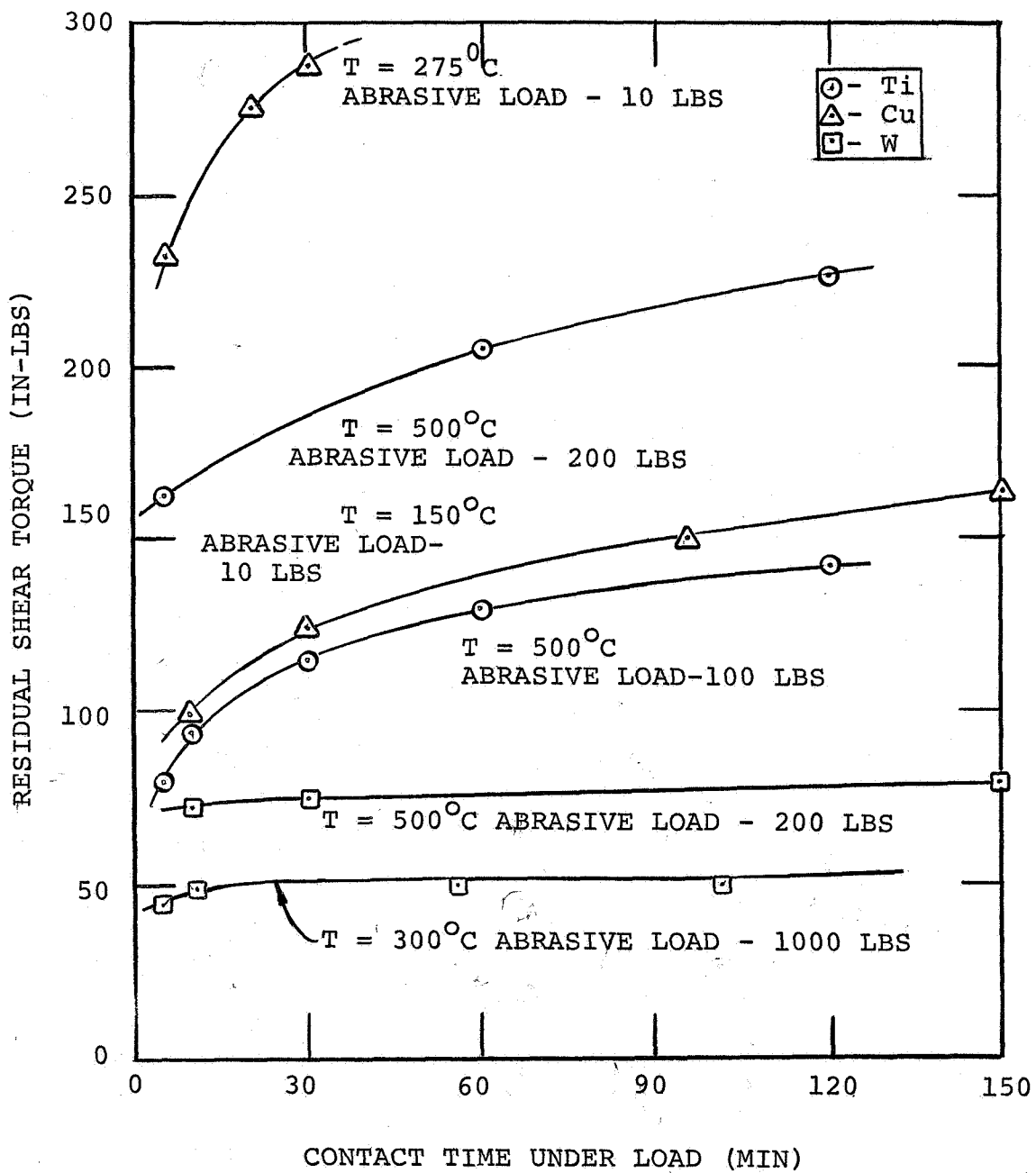


Fig. 19. Time-temperature dependence of the residual adhesion torque after 1000 lbs loading.

mechanism as a Rutherford "hard sphere" collision process, values of the sputtering yield S , defined as the ratio of ejected surface atoms to the incident ions, have been determined for Xe^+ ions. Assuming an incident ion energy of $\sim 1000\text{eV}$, $S \sim 0.5$ for titanium and tungsten and ~ 3 for copper.⁶ Thus the estimated unit sputtering rate would be $\sim 3 \times 10^{10}$ atoms/ cm^2 -sec. for Ti and W and $\sim 1.9 \times 10^{11}$ atoms/ cm^2 -sec. for copper.

For comparison, the unit gas adsorption rate may be calculated for the system. For planar surfaces, the adsorption rate γ is:

$$\gamma = 3.5 \times 10^{22} \alpha P / (MT)^{1/2} \text{ atoms/cm}^2 \text{ sec.} \quad (3)$$

where P is the gas pressure at the surface in torr units, T is the absolute temperature, M is the atomic weight of the absorbed species and α is sticking coefficient. Assuming that the adsorbed species of interest is oxygen, the critical partial pressure of oxygen at which the adsorption rate equals the sputtering rate is about 8×10^{-11} torr for tungsten and titanium and about 5×10^{-10} torr for copper, taking the values $T=300^\circ\text{K}$, $M=32$ and α as unity. With a total system pressure originally of about 5×10^{-10} torr, it is estimated that the oxygen partial pressure would be safely below the critical levels, and the sputtering rate would exceed the re-adsorption rate.

Rotary Abrasion Tests

The results of the adhesion or zero load shear torque tests after rotational abrasion on copper, titanium and tungsten suggest that the ease of welding is related to surface sensitive properties such as the metal oxide coating stability, crystallographic structure as well as mechanical properties such as ductility and yield strength. For cubic metals with relatively low oxide formation energies such as Cu and W, the adhesion shear force decreased with yield strength in agreement with previous investigations. For example, in the present tests, for an equivalent 1000 lbs load, the adhesion shear torque at zero load decreased by a

factor of two comparing copper to tungsten. The relative hardness values for the two metals also vary by a factor of approximately two.

In the case of titanium, however, other parameters in addition to plasticity have to be considered. Titanium forms a strongly adherent tenacious oxide which can only be removed with difficulty. At room temperature, it also has the hexagonal (HCP) crystal structure with lower-co-ordination number than the cubic (FCC) or (BCC) structures. It may be expected, therefore, that welding will be severely limited despite the relative softness of the metal. The experimental results appear to bear this out.

In the present work, the shear torque values have not been converted to shear stresses due to the uncertainty in estimating the actual contact area. From measurements of the wear tracks after rotation, the radial contact zone varied from as much as 2.0 cm² for copper after extended abrasion to about 0.4 cm² for titanium and tungsten. The nominal compressive stress was in the range 2000 to 65,000 psi for 1000 lbs load application.

Effect of Temperature on Adhesion Shear Forces

It was evident from the experimental results that the effect of temperature was to substantially improve the adhesion of copper and titanium. However, tungsten was only moderately affected in the range up to 500°C. The adhesion improvement with temperature for Cu and Ti may be attributed partially to the thermal relaxation of the mechanical strength, thus permitting greater plastic deformation at the specimen surface, and partially to thermal diffusion bonding. The effect of surface film contamination was also observed to be an important factor. Increased abrasive loads and rotation periods substantially improved the disruption and removal of surface oxides, thus allowing increased metallic contact. At the higher temperatures, surface abrasion was extended to a larger area of contact due to plastic flow with the result that a greater amount of clean contact area was available for welding. It may be surmized that extensive plastic surface flow considerably aids in disrupting the

Contaminant films and producing bare metal contact surfaces.

It is of interest to note that considerable welding occurred at temperatures as low as 150°C for copper and 275°C for titanium even for contact load times of 5 minutes. Thus, welding may be expected for these materials even in the absence of substantial diffusion-enhanced bonding. The ability of copper to self-adhere at relatively low temperatures has been well established and has been attributed to the relative ductility of the metal and the ease of removal of copper oxide.

The ability of titanium to self-adhere at moderately elevated temperatures can be attributed chiefly to the thermal relaxation of the mechanical strength. The yield strength of annealed titanium decreases from about 60,000 psi at 20°C to about 16,000 psi at 500°C. Thus at the higher temperatures, the applied compressive force will generally exceed the yield and satisfy the ductility requirement for welding. Measurement of the circular contact zone formed during abrasion and compression in titanium showed that the maximum nominal contact area was about 0.035 in². For the full compressive load of 1000 lbs, the resultant nominal stress over the contact zone would be about 28,500 psi. Since the yield strength of Ti is less than 25,000 psi at temperatures above 260°C, it is apparent that the contact zone will plastically deform above 260°C. Thus large scale welding may be expected in this load-temperature range.

In the case of tungsten, an exceedingly hard metal, the imposed surface stresses generally did not exceed the bulk yield stress, thus plastic deformation at the interface was quite limited. The relative insensitivity of tungsten self-adhesion with temperature may be attributed to the limited degree of thermal relaxation. It was observed that tungsten specimens tended to rupture or spall at the contact surface under high abrasive loads even at 500°C, indicating the limited capacity of ductile flow. However, since tungstic oxides have lower heats of formation than titanium oxides, the initial adhesion forces were frequently higher than for titanium due to the relative ease in preparing contaminant-free surfaces.

Summarizing the experimental data for the abrasive cleaning technique, zero-load torque tests show that:

1. Copper showed the highest degree of adhesion strength at all temperatures due to its ductility and ease of oxide removal.
2. At low temperatures, tungsten gave higher adhesion forces than titanium due to the relative ease of oxide removal and larger number of intrinsic unit atomic bonds.
3. At higher temperatures, larger bonding forces were obtained with titanium compared to tungsten due to the mechanical softening and plastic flow of the former.

Frictional Effects

It was observed that the frictional resistance to rotational shear increased in the direction titanium-tungsten-copper. At 20°C, the friction coefficients of titanium and tungsten were about 0.6 and 0.8 respectively. The friction coefficient for copper was estimated to exceed 1 for the test conditions. The trend of the coefficients may be attributed to the relative efficiencies of the metallic oxides acting as boundary lubricants.

At elevated temperatures, the friction coefficient of tungsten decreased slightly. This result may be related to the increased brittleness observed with increase in temperature. In particular, rotation under load was observed to produce fine powder particles ground from the contact surfaces. Brittle fracture and spalling would be expected to shear localized weldments and provide reduced resistance to slip. For titanium, the coefficient of friction was largely insensitive to the temperature since the increased area of contact generally compensated for the decrease in metallic strength.

CONCLUSIONS

In analyzing the results of the present investigation, the following conclusions may be drawn.

1. Substantial adhesion forces, determined either as a shear torque or a normal rupture force, may be generated in engineering metals provided the contact surface is oxide-free and a compressive force sufficient to cause extensive plastic flow at the interface is applied.

2. Assuming the presence of clean surfaces, the controlling parameter in metallic bonding is, generally, the yield strength or ductility of the metal. Hard metals, such as tungsten, will only weld with difficulty at low temperatures due to high elastic stresses at the interface.

3. Welding will increase in proportion to the degree of surface cleanliness and to the area of contact.

4. Adhesion forces, under equivalent conditions, will increase with temperature and time due to the contributing effects of diffusion bonding and to the decrease in mechanical strength.

5. Frictional effects in vacuum are chiefly controlled by the tenacity of the metal oxide film acting as a boundary lubricant and probably also by the lattice structure. Hence BCC tungsten yielded a higher coefficient of friction in vacuum than HCP titanium.

6. For titanium, the friction coefficient is largely independent of temperature, the coefficient for tungsten decreased with temperature due to enhanced metallic brittleness with sliding stresses.

7. The ion bombardment method for stripping surface contaminant films is at least partially useful for producing large scale bonding. The abrasive cleaning treatment was found to generate large adhesion forces presumably due to the larger area of contact formed.

FUTURE WORK

With regard to the phenomena of metallic adhesion and friction as a possible problem in space operations, several areas may be fruitfully studied. These include:

1. The influence of changes in the mechanical properties such as yield strength and plastic strain caused by metallurgical treatments.
2. The effect of surface geometry and the influence of the amount of interfacial contact area.
3. The variation of adhesion-friction forces with alloy type and crystallographic lattice structure.
4. The effect of surface micro-contour or finish.
5. The effect of residual atmospheres of reactive gases or liquids acting as boundary lubricants or as reaction agents to change the nature of the surface films. From the results of the present work, it is apparent that surface adsorbed films vary in their tenacity or bonding energy. Changes in film strength may vitally effect the relative ease of film removal under abrasive contact or particle bombardment.

With respect to contaminant film removal techniques and the preparation of clean surfaces, an interesting and important field of study is particle impingement as exemplified by ion sputtering. In extended space operations, exposed surfaces will be continuously irradiated by a cosmic particle stream which may be quite effective in removing boundary surface layers. Studies under NASA Contract NAS1-2691, Task 5 in this series of programs and in the present work have shown that surfaces can be cleaned by incident particles with the proper energy and density distributions sufficient to cause enhanced bonding and friction.

Future work in this area should include:

1. Quantitative estimates of the amount of surface film removal by changes in the electron work function as a function of particle impingement density and energy.

2. The effect of various oxide formation or bonding energies on the degree or severity of particle bombardment necessary to produce oxide film sputtering.

REFERENCES

1. Bowden, F.P.: The Adhesion of Metals and the Influence of Surface Contamination and Typegraphy. Ed. Weiss, P.: Adhesion and Cohesion. Elsevier Pub., New York, 1962.
2. Milner, D.R. and Rowe, G.W.: Fundamentals of Solid Phase Welding. Metal. Rev., vol.7, no.28, 1962, pp.433-480.
3. Bowden, F.P. and Rowe, G.W.: The Adhesion of Clean Metals. Proc. Roy. Soc., vol.233, ser. A, 1956, pp. 429-442.
4. Ham, J.L.: Metallic Cohesion in High Vacuum. Trans. Amer. Soc. Lub. Engrs., vol.6, 1963, pp. 20-28.
5. Kaminsky, M.: Atomic and Ionic Impact Phenomena on Metal Surface. Academic Press, New York, 1965, pp.151-153.
6. Ibid.: pp.153-156.